minerals

MDPI

Review

Fertility Indicators for Porphyry-Cu-Au+Pd±Pt Deposits: Evidence from Skouries, Chalkidiki Peninsula, Greece, and Comparison with Worldwide Mineralizations

Maria Economou-Eliopoulos [1,*], Federica Zaccarini [2] and Giorgio Garuti [2]

[1] Department of Geology and Geoenvironment, University of Athens, 15784 Athens, Greece
[2] Brunei Darussalam, Jalan Tungku Link, Gadong, Bandar Seri Begawan BE1410, Brunei; federicazaccarinigaruti@gmail.com (F.Z.); giorgio.garuti1945@gmail.com (G.G.)
* Correspondence: econom@geol.uoa.gr

Abstract: The research interest for many authors has been focused on the origin, recovery, and exploration of critical metals, including platinum-group elements (PGEs), with the aim of finding new potential sources. Many giant porphyry Cu deposits are well known around the Pacific Rim, in the Balkan–Carpathian system, Himalayas, China, and Malaysia. However, only certain porphyry Cu-Au deposits are characterized by the presence of significant Pd and Pt contents (up to 20 ppm). This contribution provides new analytical data on porphyry-Cu-Au±Pd±Pt deposits from the Chalkidiki Peninsula and an overview of the existing geochemical characteristics of selected porphyry-Cu deposits worldwide in order to define significant differences between PGE-fertile and PGE-poor porphyry-Cu intrusions. The larger Mg, Cr, Ni, Co, and Re contents and smaller LILE elements (Ba and Sr) in fertile porphyry-Cu-Au-(PGE) reflect the larger contribution from the mantle to the parent magmas. In contrast, the smaller Mg, Cr, Ni, Co, and Re contents and larger Ba and Sr in PGE-poor porphyry-Cu-Mo deposits from the Chalkidiki Peninsula (Vathi, Pontokerasia, and Gerakario) and Russia–Mongolia suggest the presence of parent magmas with a more crustal contribution. Although there is an overlap in the plots of those elements, probably due to the evolution of the ore-forming system, consideration of the maximum contents of Mg, Cr, Ni, and Co is proposed. Magnetite which separated from the mineralized Skouries porphyry of Greece showed small negative Eu anomalies ($Eu/Eu^* \geq 0.55$), reflecting a relatively high oxidation state during the cooling of the ore-forming system. The relatively high, up to 6 ppm (Pd+Pt), and low Cr content towards the transition from the porphyry to epithermal environment, coupled with the occurrence of Pd, Te, and Se minerals (merenskyite, clausthalite), and tetrahedrite–tennantite in fertile porphyry Cu deposits (Elatsite deposit, Bulgaria), reflect a highly fractionated ore-forming system. Thus, in addition to the crustal and mantle recycling, metasomatism, high oxidation state, and abundant magmatic water, other factors required for the origin of fertile porphyry-Cu deposits are the critical degree of mantle melting to release Pt and Pd in the ore-forming fluids and the degree of fractionation, as reflected in the mineral chemistry and geochemical data.

Keywords: porphyry; palladium; platinum; potential; magnetite; fertility; exploration

Citation: Economou-Eliopoulos, M.; Zaccarini, F.; Garuti, G. Fertility Indicators for Porphyry-Cu-Au+Pd±Pt Deposits: Evidence from Skouries, Chalkidiki Peninsula, Greece, and Comparison with Worldwide Mineralizations. *Minerals* **2023**, *13*, 1413. https://doi.org/10.3390/min13111413

Academic Editors: Liqiang Yang and Nuo Li

Received: 9 August 2023
Revised: 25 October 2023
Accepted: 2 November 2023
Published: 6 November 2023

1. Introduction

In recent decades, the exploitation of primary raw materials has rapidly increased worldwide due to the continuous growth of the global population and technological innovations [1,2]. The research interest for many authors has been focused on the origin and exploration of new sources for critical and strategic raw materials, including platinum-group elements (Os, Ir, Ru, Rh, Pt, Pd) or PGE. Among the PGE, Pt and Pd are the most economically relevant due to their use in electronics, jewelry, medical applications, and in the catalytic converter of vehicles to reduce the pollutants of exhaust gases [3–6]. With few exceptions that consist of placer deposits, economic PGE deposits occur in mineralized

horizons associated with mafic–ultramafic igneous rocks. Presently, about 90% of Pt and Pd production comes from two countries, South Africa (the Merensky Reef, Platreef and Upper Group 2 (UG2) stratiform chromitites) and the largest Pd deposit in the world, occurring in sill-like intrusions enriched in Cu-Ni magmatic sulfides associated with flood basalts, in the Norilsk intrusion of Russia [7]. The chromitites associated with ophiolite complexes, containing significant amounts of Pt, Pd, and Rh, represent only 7% of the investigated podiform chromitites; therefore, they are not presently considered to be a potential resource due to their local enrichment and the small size of the PGE-enriched chromitite bodies [6].

Many giant porphyry Cu-Au, Cu-Mo, and Mo-W deposits extend from the Pacific Rim to the Mediterranean and Carpathian system in Europe, the Himalayas, China, and Malaysia. However, only certain porphyry Cu-Au deposits, associated mostly with alkaline-type intrusions, are characterized by significant Pd and Pt contents, particularly in high-grade bornite–chalcopyrite and/or flotation concentrates. Such porphyry deposits include those in British Columbia, Colorado [8,9], in the Santo Tomas II deposit, the Philippines [10], the Skouries porphyry deposit, Greece, Elatsite, Bulgaria [11–13], the Kalmakyr deposit, Uzbekistan [14], the Grasberg deposit, Indonesia, Ok Tedi, Papua New Guinea, the Mamut deposit, Malaysia, and the Bajo de la Alumbrera, Argentina [15–19]. Case studies on PGE-rich porphyry-Cu systems have shown that high PGE contents (up to ppm levels of Pt and Pd) may also occur in the magnetite-bearing assemblages of potassic alteration zones, representing the early high temperature stages from an underlying magma reservoir into the porphyry system, dominated by magmatic–hydrothermal fluids as Cl-complexes [19,20]. A few porphyry-Cu deposits contain potentially economic concentrations of PGE. Palladium and lesser Pt have been recovered from Majdanpek and Bor deposits, located in Serbia [21], and in a number of gold deposits, including the giant Cu-Au-Mo porphyry deposit of Kalmakyr in Uzbekistan [14]. The New Afton deposit of British Columbia contains potentially economic concentrations of PGE, up to 21 ppm Pd and 230 ppb Pt, with an average contents of 720 ppb Pd and 35 ppb Pt (n = 160) [22]. Some porphyry Cu-epithermal gold deposits are also considered to be potential sources of PGE as by-products [20,23]. However, further exploration is required to evaluate if the PGE potential is high enough to become a future major source of PGE [20], and to find a possible model responsible for the enrichment of precious metals that may include the partial melting of metasomatized lithospheric mantle, partial re-melting of sulfide-bearing cumulates, oxygen fugacity at the mantle source region, or fractional crystallization [10–23]. Also, the fertility of the porphyry Cu-Au-Pd-Pt deposits and the mechanism permitting the transfer of these elements from the mantle to the magma source for porphyry–epithermal deposits still remain unclear [22,24,25]. In this contribution, we have selected the Skouries porphyry-Cu-Au±Pd±Pt deposit and the (Pd-Pt)-poor porphyry-Cu-Mo deposits of Vathi, Pontokerasia, and Gerakario, all hosted in the Vertiskos Formation of the Serbo-Macedonean Massif (SMM) of Greece, in a worldwide comparative study, including some porphyry-Cu-Au±Pd±Pt and PGE-poor deposits, aiming to improve the knowledge of the future exploration and exploitation of PGE in calc–alkaline hydrothermal systems.

2. Materials and Methods

2.1. Sampling

The geochemical characterization of the porphyry-Cu mineralization from the Skouries deposit is based on the data from the surface and half core and quarter core of drill holes collected during the exploration project by the TVX Hellas S.A. (now Eldorado Gold Corporation (Vancouver, British Columbia, Canada) acquired European Goldfields Ltd.)) (Figure 1), reaching a depth > 600 m, as provided in previous publications [11–14] and the present study (Tables 1–3).

2.2. Analytical Methods

Some more electron microprobe and whole rock analyses for major trace and ultra-trace elements from the Skouries deposit are presented (Tables 1–3) in order to compare with

the existing data on representative samples from other porphyry-Cu deposits worldwide. These samples were analyzed by inductively coupled plasma mass spectroscopy (ICP/MS) after hot aqua regia digestion at the ACME Analytical Laboratories Ltd., Vancouver, BC, Canada. In addition, selected large (weighting approximately 2 kg) porphyry-Cu samples, representative of increasing depth from 43 to 635 m, were used for the separation of disseminated magnetite. These samples were crushed and pulverized in an agate mortar. The multi-stage water flotation was applied, and magnetite separates were concentrated magnetically. This portion was furthermore pulverized in the agate mortar at a size fraction < 75 μm, and magnetite separates were separated furthermore from silicates, and they were analyzed for minor and trace elements (Table 2) after sodium peroxide fusion, combined with inductively coupled plasma and atomic emission spectroscopy (ICP-AES), at the SGS Analytical Laboratories Ltd., Vancouver, BC, Canada.

The Pd, Pt, and Au were determined by ICP-MS analysis after pre-concentration using the Lead Fire Assay technique from large (30 g) samples of mineralized rocks at the Acme Laboratories Ltd., Vancouver, Canada (Table 3). Detection limits are 1 ppb for Pd and Au, 10 ppb for Pt.

Polished sections of mineralized porphyry-Cu samples were examined via reflected light microscopy and a scanning electron microscope (SEM) using energy-dispersive spectroscopy (EDS). SEM images and EDS analyses of sulfides and oxides were carried out at the University of Athens (Department of Geology and Geoenvironment, Athens, Greece), using a JEOL JSM 5600 scanning electron microscope, equipped with the automated energy-dispersive analysis system ISIS 300 OXFORD with the following operating conditions: accelerating voltage 20 kV, beam current 0.5 nA, time of measurement 50 secs, and beam diameter 1–2 μm. The following X-ray lines were used: OsMα, PtMα, IrMβ, AuMα, AgLα, AsLα, FeKα, NiKα, CoKα, CuKα, CrKα, AlKα, TiKα, CaKα, SiKα, MnKα, MgKα, ClKα. The standards used were pure metals for the elements Os, Ir, Rh, Pt, Pd, Au, Ag, Cu, Ni, Co, Ti, Mn, Zr, Hf, and Cr, indium arsenide for As, Pyrite for S and Fe, SiO_2 for Si, ThO_2 for Th, MgO for Mg, Al_2O_3 for Al, Wollastonite for Ca, NaCl for Cl, and GaP for P.

3. Characteristic Features of the Skouries and Other Porphyry-Cu-Au+Pd±Pt Deposits

3.1. Geological Outline

The progressively collisional subduction of Tethys has led to mineralized ophiolitic slabs thrust over onto the Paleozoic continental margin of the Serbo-Macedonian massif (SMM) basement rocks and generated intra-continental syn-orogenic faults, which facilitated extensive Tertiary magmatic plutonic and sub-volcanic rocks, including porphyry Cu-Au intrusions [26,27]. The Skouries Vathi, Pontokerasia, and Gerakario porphyry-Cu intrusions belong to the Vertiskos unit of the SMM, extending to Serbia and Bulgaria (Figure 1; [28–31]).

The Vertiskos unit, at the central part of the SMM, is composed of an alternation of gneisses and schists, hosting mafic–ultramafic bodies (ophiolites) of Jurassic age, known as the Gomati–Therma–Volvi (GTV) complex, which has been metamorphosed to high-grade amphibolite facies [28,32–35]. Calc–alkaline magmatism started in the Early Miocene (22–17 Ma) is characterized by the intrusion of several subvolcanic rocks that host porphyry-style mineralization, including Vathi, Pontokerasia, Gerakario, and Skouries [36,37]. Based on whole-rock SiO_2 and alkali, the Skouries intrusion can be classified as a high K calc–alkaline type [11,18,34]. Also, although the contents of trace elements are scattered over a wide range, the high K/Rb and low Rb/Sr ratios from the Skouries porphyry stock are similar to PGE-fertile porphyry at the Allard stock, La Plata Mountains Colorado [8,9,11].

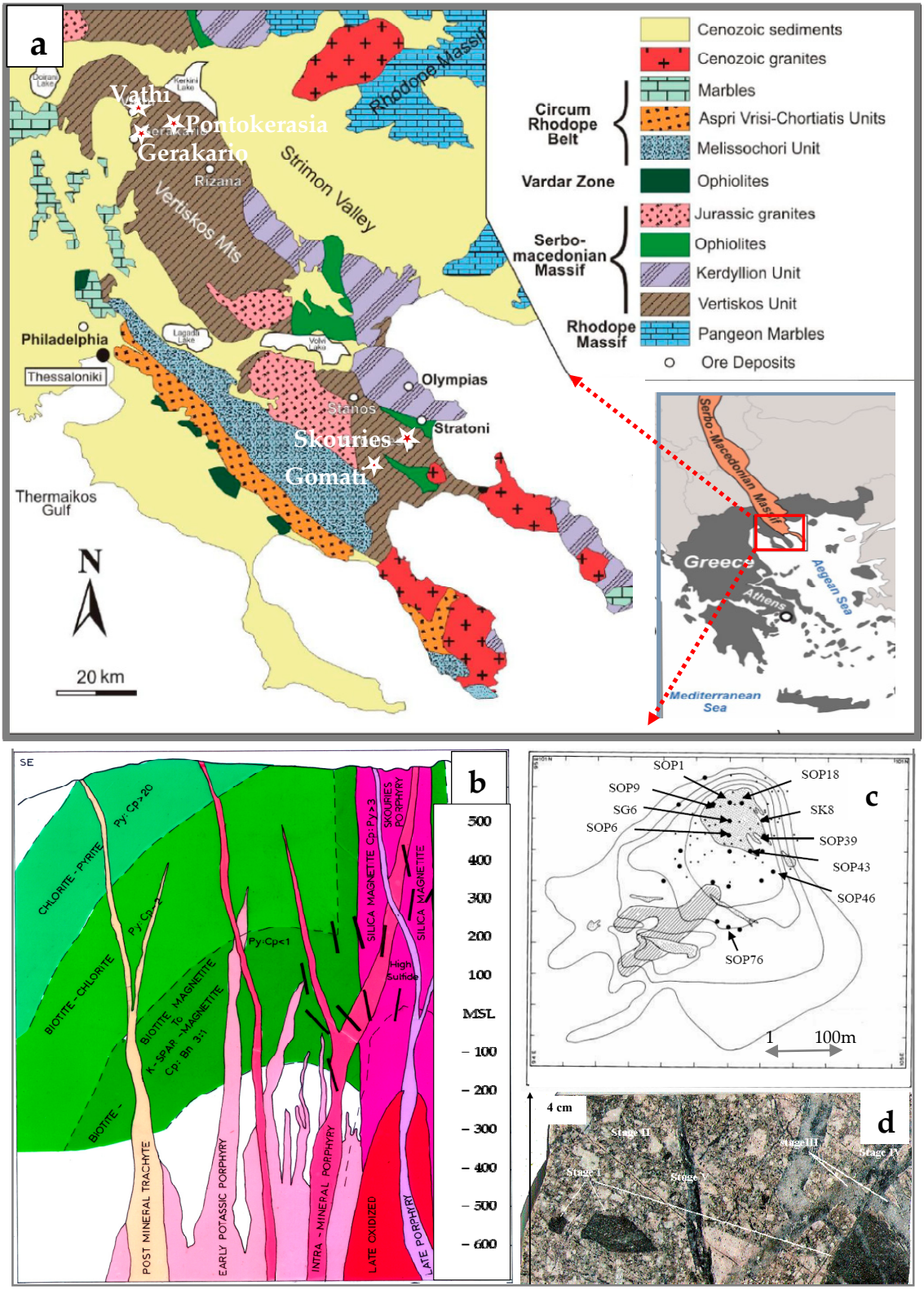

Figure 1. (**a**): Simplified geology of the Serbo−Macedonian Massif the studied part is marked by the red frame (modified after [30,31]); (**b**): schematic cross−section showing crosscutting successive monzonite porphyry intrusions; (**c**): the location of drill holes in the Skouries porphyry deposit [29]; (**d**): representative drill core sample, showing the presence of dark-green angular mafic fragments to a sharp contact with the host porphyry, and crosscutting relationships between successive quartz veins. Abbreviation: Cp = chalcopyrite, Py = pyrite, K-SPAR = K-feldspar.

Three major fault groups characterize the regional structures, which controlled the emplacement of the intrusions in the crystalline basement of the Vertiskos Unit. Based on crosscutting and overprinting relationships, at least four stages of mineralization have been described in the porphyry Cu-Au deposit of Skouries (Figure 1b): (1) the initial quartz monzonite porphyritic phase and (2) the main stage of porphyritic syenite, associated with the mineralization of defined reserves approximately 205 Mt at 0.5% Cu, and 0.53 ppm Au, (3) the porphyritic mela-syenite dykes, and (4) the late stage, which crosscuts all earlier phases [18,29,32,33,38,39]. According to these authors, magnetite–chalcopyrite (reaching up to 10 vol.%, average 6 vol.%) and bornite–chalcopyrite, linked to a pervasive potassic and propylitic alteration, crop outs in the central parts of the deposit, while chalcopyrite–pyrite dominates around the periphery of the deposit. Molybdenite is rare and occurs in pyrite–sericite–carbonate-bearing veinlets at the marginal parts of the deposit, with only a minor quantity of chalcopyrite.

The presence of isolated fragments of dark-green mafic fragments in drill core samples has been noted (Figure 1d) [13,19]. In addition, drill-hole samples from a depth of more than 300 m contain relatively large fragments of metamorphosed basic rocks, intruded by porphyry intrusions that affect the sulfide mineralization (Figure 2).

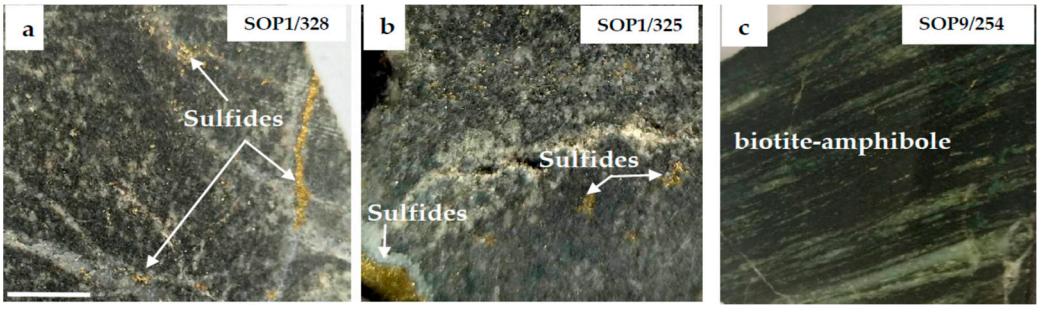

Figure 2. Photographs of dark-green biotite–amphibole metamorphic country rocks, which are dominant in drill cores as xenoliths in the Skouries porphyry. (**a**,**b**): Sulfide mineralization in those rocks intruded by porphyry intrusions are common. (**c**): layered amphibolite. Bar scale (**a**–**c**) = 1 cm.

A calc–alkaline syenite and a quartz granodiorite intrusion host the Vathi, Gerakario, and Pontokerasia porphyry deposits in SMZ are of Miocene age (18 Ma) too, with more than 258 Mt of ore at 0.40 wt.% Cu and 0.9 g/t Au [36].

3.2. Mineralogical Characteristics

New data presented here are combined with those available from previous detailed descriptions on the porphyry deposits hosted in the Vertiskos Formation [11,13,18,19,36–39]. Magnetite–chalcopyrite ± bornite, linked to pervasive potassic and propylitic alteration, is exposed in the central parts of the Skouries deposit, while pyrite, that is dominant around the periphery of the deposit, is characterized by a significant (Ni±Co) content, for example, those from the SOP76 drill-hole (Figure 1c) (Table 1). The hypogene mineralization at the Vathi occurs in the quartz monzonite, while the potassic alteration is associated with vein-type ore assemblage: pyrite + chalcopyrite + bornite + molybdenite + magnetite, the propylitic alteration is related to pyrite + chalcopyrite, and the sericitic alteration is associated with the assemblage pyrite + chalcopyrite + native gold ± tetradymite. The assemblage sphalerite + galena + arsenopyrite + pyrrhotite + pyrite ± stibnite ± tennantite is related to a subsequent epithermal overprinting event [36].

Table 1. Selected characteristics of the porphyry-Cu deposits from the Chalkidiki Peninsula.

Deposit	Setting	Age	Affinity	Drill Hole	Location of Drill Hole	Alteration	Mineralization	Mineralogy
Skouries	Col	18 Ma	Monzonite syenite	SOP06 SG6	Central part	Potassic	ccp-mgt±bn minor: native Au-mrk-hes-syl-zrn	qz-or-ab-an-bt-phl-ap
				SOP18 SOP1 SOP09	Proximal to center	Potassic	ccp-mgt±bn minor: native Au-me-zrn-thr	qz-or-ab-an-bt-phl-ap
				SK8 SOP39 SOP43	Peripheral part	Potassic and clay	ccp-py-mol-mgt	qz-or-ab-bt-phl-ap-cal
				SOP46 SOP76	Marginal part	Potassic and clay	ccp-py-cc-mol-mgt ccp-py-sp-gn	qz-ab-ms-ser-cal
Vathi, Gerakario, Pontokerasia	Col	18 Ma	Quartz monzonite syenite	Surface samples		Potassic Propylic	py-ccp-mol-mgt py-ccp-mol-cc-apy	qz-or-ab-an-bt-ser-cal
						Sericitic	py-ccp-cc-sp-gn	

Abbreviations: SMM = Serbo-Macedonian Massif; Col = during or following collision; ccp = chalcopyrite, mgt = mgnetite, bn = bornite, mrk = merenskyite, hes = hessite, syl = sylvanite, zrn = zircon, thr = thorite, py = pyrite, mol = molybdenite, cc = chalcocite, sp = sphalerite, gn = galena, apy = arsenopyrite, qz = quartz, or = orthoclase, ab = albite, an = anortite, bt = biotite, phl = phlogopite, ap = apatite; cal = calcite, ms = muscovite.

Table 2. Representative electron microprobe analyses of minerals from porphyry-Cu deposits of the Balkan Peninsula, present study; (*) [16,40]; n.d. not detected.

Country	Greece							Bulgaria *				
Deposit Drill-hole	Skouries SOP-76	SOP-76	SOP-76	SOP-76	SOP-46	SG-6	SG-6	Elatsite n = 4	Elatsite n = 4	Medet	Medet	Medet
Mineral	pyrite	pyrite	pyrite	pyrite	pyrite	pyrite	pyrite	linnaeite	siegenite	Pyrite	Pyrite	Carrolite
wt.%												
Fe	45.6	45.6	46.5	42.6	45.6	46.2	43.4	1.4	3.4	38.2	33.8	1.8
Cu	n.d.	n.d.	n.d.	n.d.	n.d.	0.4	n.d.	16.3	3.3	0.1	0.1	15.9
Ni	0.9	0.9	1.1	4.2	1.9	0.7	n.d.	7.4	34.7	5.3	0.4	3.2
Co	0.6	0.6	n.d.	n.d.	0.5	n.d.	n.d.	34.4	17.3	2.2	12.4	37.6
As	n.d.	n.d.	n.d.	n.d.	n.d.	n.d.	0.9	n.d.	n.d.	n.d.	n.d.	n.d.
Au	n.d.	n.d.	n.d.	n.d.	n.d.	n.d.	4.8	n.d.	n.d.	n.d.	n.d.	n.d.
S	52.6	52.6	53.3	52.2	52.5	51.9	50.7	41.3	41.5	53.9	53.2	41.6
Total	99.7	99.7	100.9	99	100.5	99.2	99.8	100.8	100.2	99.7	99.9	100.1

Table 2. *Cont.*

Drill-hole	SK8	SOP18	SOP18	SG-6	SOP76	SOP18	SOP43	SOP18	SOP18	SK8	SK8	SK8
Mineral	Zircon	Core Zircon	Rim Zircon	Cl-(OH) Apatite	Cl-(OH) Apatite	Rutile	Thorite	U-thorite	U-thorite	Ti-Magnetite	Cr-bearing Magnetite	
SiO_2	32.6	31.3	31.7	n.d.	n.d.	0.4	18.8	15.6	15.2	0.2	0.3	0.7
Al_2O_3	n.d.	n.d.	n.d.	n.d.	n.d.	0.3	n.d.	n.d.	n.d.	n.d.	n.d.	n.d.
Cr_2O_3	n.d.	n.d.	n.d.	n.d.	n.d.	n.d.	n.d.	n.d.	n.d.	n.d.	0.7	0.8
TiO_2	n.d.	n.d.	n.d.	n.d.	n.d.	95.5	n.d.	n.d.	n.d.	19.8	n.d.	n.d.
FeO	0.6	0.4	n.d.	n.d.	0.6	2.2	n.d.	0.6	4.3	49.4	31.0	30.9
Fe_2O_3	n.d.	n.d.	n.d.	n.d.	n.d.	n.d.	n.d.	n.d.	n.d.	30.8	68.2	67.6
MgO	n.d.	n.d.	n.d.	n.d.	n.d.	n.d.	n.d.	n.d.	n.d.	n.d.	n.d.	n.d.
MnO	n.d.	n.d.	n.d.	n.d.	n.d.	n.d.	n.d.	n.d.	n.d.	n.d.	n.d.	n.d.
CaO	n.d.	n.d.	n.d.	55.0	52.7	n.d.	n.d.	n.d.	n.d.	n.d.	n.d.	n.d.
P_2O_5	n.d.	n.d.	n.d.	43.9	42.5	n.d.	n.d.	n.d.	n.d.	n.d.	n.d.	n.d.
SO_3	n.d.	n.d.	n.d.	n.d.	0.4	n.d.	n.d.	n.d.	n.d.	n.d.	n.d.	n.d.
ZrO_2	67.2	65.4	68.3	n.d.	n.d.	67.2	n.d.	n.d.	n.d.	n.d.	n.d.	n.d.
ThO_2	n.d.	3.2	n.d.	n.d.	n.d.	n.d.	79.5	70.68	50.8	n.d.	n.d.	n.d.
HfO_2	n.d.	n.d.	n.d.	n.d.	n.d.	n.d.	n.d.	n.d.	n.d.	n.d.	n.d.	n.d.
UO_3	n.d.	n.d.	n.d.	n.d.	n.d.	n.d.	n.d.	11.9	29.2	n.d.	n.d.	n.d.
Total	100.4	100.3	100.0	98.9	96.2	98.4	98.3	98.78	99.5	100.2	100.2	100

Disseminated magnetite as part of the quartz–bornite–chalcopyrite assemblages in the potassic alteration zones, proximal to the centers, is a characteristic feature in the Skouries and Elatsite deposits [16–20]. Merenskyite (the most common PGE-mineral) occurs commonly as inclusions or on the edge of hydrothermal chalcopyrite [18,19,37]. More attention was paid here on the texture and mineral chemistry of magnetite (Figure 3; Table 3) in order to define significant differences compared to PGE-poor porphyry-Cu intrusions.

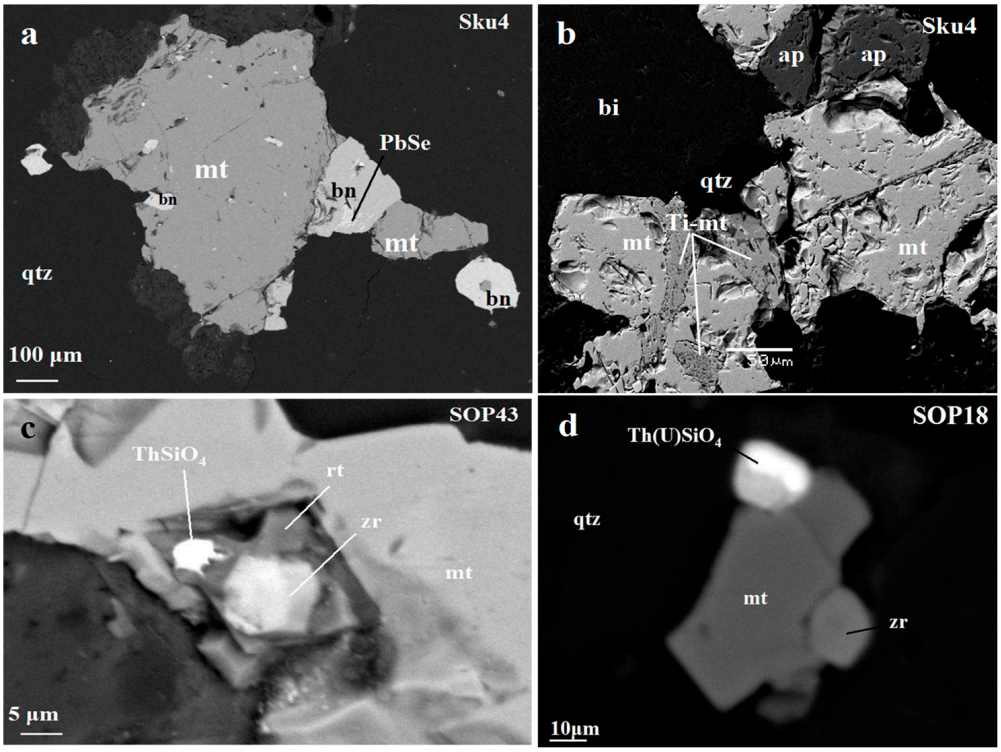

Figure 3. Backscattered electron images from drill core samples at Skouries porphyry deposit. (**a**): clausthalite and bornite intergrowths with magnetite; (**b**): magnetite intergrowths with apatite; (**c**): association of rare accessory minerals with Ti-magnetite; (**d**): uranium-rich thorite and zircon associated with Ti-magnetite within a quartz matrix. Abbreviations: mt = magnetite; bn = bornite; qtz = quartz; ap = apatite; bi = biotite; rt = rutile; zr = zircon.

Magnetite in the Skouries porphyry Cu deposit results in the occurrence of intergrowths with Ti-magnetite, ilmenite, zircon, very fine Cu minerals (bornite and chalcopyrite), thorite, U-bearing thorite, rare earth element (REE) minerals (mostly monazite) and Cl,(OH)-apatite (Figure 3; [19]. Zircon often shows zoning, with Fe, Th, Hf, and S in the core in contrast to the rim (Table 3). Uranium-rich thorite is associated with Ti-magnetite hosted by quartz (Table 1).

Separates of disseminated magnetite, derived from large porphyry-Cu samples, were analyzed for major and trace elements. The Th contents ranging from 28 to 110 ppm (mean 65), U ranging from 5.3 to 31 (mean 15 ppm), and Zr ranging from 119 to 700 ppm (mean 323) in magnetite separates are much larger than in bulk analyses and confirm their association with magnetite (Figure 3c,d). In addition, a characteristic feature of the magnetite is the relatively high Cr (average 0.8 wt.% Cr_2O_3 (Table 1), reaching up to 2.3 wt.% Cr_2O_3) in SEM/EDS analyses, and in magnetite separates, the high Cr, Ni, and Co contents reach values up to 1060 Cr, 640 Ni, and 69 Co (all in ppm, Table 2). The average Cr content in magnetite from the Vathi porphyry [37] and Cr (16 ppm) from the Pagoni Rachi Cu-Mo-Re-Au porphyry prospect, northern Greece (Thrace), was 110 ppm and 16 ppm, respectively [41], meaning that they are much lower compared to that in magnetite from the Skouries deposit (Tables 2 and 3).

Table 3. Composition of disseminated magnetite separates from the Skouries drill-holes. Present study.

	Skouries			Detection Limit	Standard OREAS684	Vathi
ID sample	SOP43/200	Porphyry-Cu SOP6/363	Skou8/280			
ppm						
As	<5	<5	<5	5	<5	52
Bi	10	5.2	5.4	0.1	0.4	
Cr	1060	560	280	0.01	13,000	240
Mn	560	430	360	0.01	1250	650
Ni	640	76	310	5	2250	300
Co	69	50	66	0.05	119	10
Cu	4850	1210	1310	0.1	960	28
Zn	61	37	68	5	95	70
V	670	920	690	1	165	3000
Ga	41	40	59	1		75
Ba	60	70	100	10	70	
La	1.2	14	2.5	2	3.4	
Ce	2.1	28	4.7	0.1	6.6	
Pr	0.2	2.8	0.5	0.1	0.74	
Nd	0.9	9.8	1.8	0.05	2.9	
Sm	0.1	1.6	0.3	0.5	0.6	
Eu	0.07	0.26	0.08	0.05	0.21	
Gd	0.16	1.2	0.3	1	0.71	
Tb	<0.05	0.16	<0.05	0.5	0.12	
Dy	0.15	0.9	0.21	0.05	0.71	
Ho	<0.05	0.2	<0.05	0.05	0.16	
Er	0.15	0.7	0.18	0.1	0.5	
Tm	<0.05	0.1	<0.05	0.05	0.08	
Yb	0.2	1.1	0.3	0.1	0.5	
Lu	<0.05	0.25	0.05	0.05	0.09	
ΣREE	4.03	46.82	8.37			
Ce/Ce*	0.95	0.98	0.96			
Eu/Eu*	1.68	0.55	0.61			
Tm/Tm*	0.19	0.79	0.47			
Sc	8	8	9	5	19	
Y	1.3	6.3	1.6	0.5	4.3	
Hf	3	18	4	1	<1	
Cs	0.7	0.2	0.2	0.1	0.2	
In	<0.2	<0.2	<0.2	0.2	<0.2	
Nb	1	7	1	1	<1	
Pb	23	16	35	0.2	13	
Rb	24	11	12	0.1	6.5	
Sb	<0.1	<0.1	<0.1	0.1	<0.1	
Sn	4	5	5	0.05	<1	
Ta	<0.5	0.6	<0.5	0.5	<0.5	
Mo	<2	<2	2	2	<2	
Li	<10	<10	<10	10	<10	
Sr	10	30	30	5	150	
Th	28	110	56	0.1	0.6	
U	5.3	31	9.3	0.5	0.2	
Zr	119	700	150	0.5	14.7	
W	74	39	52	0.1	<1	
Tl	0.5	<0.5	<0.5	0.5	<0.5	
wt%						
Si	3.7	2.8	3.4	0.01	21.1	
Al	0.58	0.54	0.6	0.01	5.75	
Fe	>25	>25	>25	10	7.99	
Ti	0.16	0.35	0.24	0.01	0.13	
Ca	<0.1	<0.1	<0.1	0.1	4.2	
Mg	0.24	0.07	<0.01	0.01	10.4	
K	0.4	0.3	0.3	0.01	0.1	
P	<0.01	<0.01	<0.01	0.01	<0.01	

The rare earth element (REE) content of magnetite separates is relatively low, and the chondrite-normalized REE patterns (Figure 4a) are similar to those for porphyry (Figure 4b)

in terms of highly fractionated LREE [42]. Mean ratios for Ce/Ce* = 0.96 and Eu/Eu* = 0.95 were calculated according to [43] (Table 3).

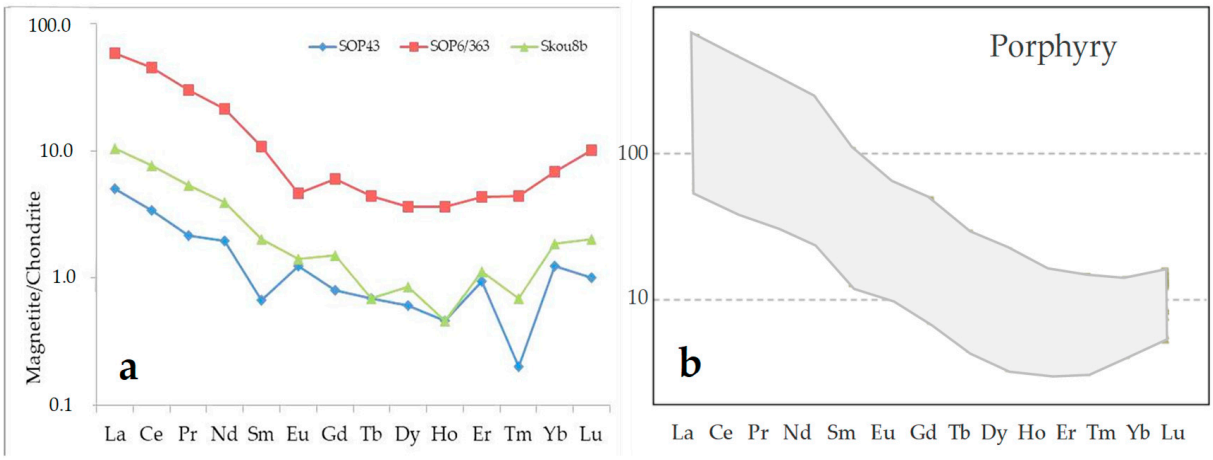

Figure 4. Chondrite normalized diagrams (**a**): for magnetite separates, data from Table 2; (**b**): for the Skouries porphyry after [42]. Chondrite values from [44].

3.3. Platinum-Group Minerals (PGMs) in the Porphyry-Cu-Au+Pd±Pt Deposits

Consistently with the geochemical data, the presence of discrete platinum-group minerals (PGMs) of Pd and, to a lesser extent, of Pt have been described in several porphyry-Cu-Au+Pd±Pt deposits, including the Skouries. In the Afton and Mt Milligan deposits of British Columbia, pyrite contains small amount of Pd [18,22,45,46]. In the Cu-sulfides associated with potassic alteration of the Skouries deposit, intergrowths of merenskyite [(Pd,Pt)(Te,Bi)$_2$], hessite (Ag_2Te), electrum, and Cu minerals (bornite and chalcopyrite) have been described [39]. More recently, the PGM identified in PGE-enriched porphyry deposits consist exclusively of Pd minerals such as merenskyite that rarely contains up to 3 wt% Pt [18]. Isomertierite ($Pd_{11}Sb_2As_2$), kotulskite [Pd(Te,Bi)], naldrettite (Pd_2Sb), sobolevskite (PdBi), sopcheite ($Ag_4Pd_3Te_4$), telargpalite [(Pd,Ag)$_3$Te)], and testibiopalladite [PdTe(SbTe)] are less abundant. The PGMs of Skouries have been identified to be enclosed or at the edge of sulfides, such as chalcopyrite and bornite, or associated with hydrothermally alternated silicates [18].

Moncheite [(Pt,Pd)(Te,Bi)$_2$], merenskyite, and kotulskite accompanied by Ag-tellurides and selenides have been described within the main magnetite–bornite–chalcopyrite assemblages of the potassic core at the Santo Tomas II (Philippines) porphyry-Cu intrusion [10], while stibiopalladinite [Pd_5Sb_2] and vysotskite [(Pd,Ni)S] have been identified in sulfide concentrates from the same deposit [47]. In addition to Ni-Co sulfides, the Elatsite deposit contains mostly mineral of the merenskyite–moncheite series accompanied by Ag-tellurides, selenides, and bismuthides [16,17,48]. In the Serbian deposit of Majdanpek, in the deposit of Mamut located in Malysia, in Mt Milligan B.C. and elsewhere the PGMs identified were merenskyite and sperrylite ($PtAs_2$) [15,49–52]. Sulfide concentrates from the Aksug deposit (Russia) contain only Merenskyite [49]. Several PGMs, such as arsenopalladinite [$Pd_8(As,Sb)_3$], kotulskite, merenskyite, naldrettite, and sopcheite, occur in the Malmyzh porphyry-Cu deposit of the Russian Far East [50].

3.4. Platinum and Palladium Distribution

Any systematic variation between the Pd and Pt contents with the drill-hole depth and the location of the drill-hole is not obvious. However, it seems likely that the maximum (Pd+Pt) contents were measured in the central part of the ore body (Figure 1c), for example, in the drill-hole labeled as SG6, whereas they are much lower in marginal drill-holes. In general, a common feature of the Skouries deposit and other (Pd, Pt, Au)-fertile porphyry-Cu deposits is the occurrence of the quartz–bornite–chalcopyrite assemblages in the potas-

sic alteration zones, proximal to centers, during the primary hypogene mineralization event [10–19,51]. A relatively high PGE content in the Skouries porphyry-Cu deposits (up to 2.4 ppm Pd in chalcopyrite concentrates) measured in vein-type highly mineralized portions from drill-hole samples, covering deeper parts of the whole mineralized porphyry of Skouries (Figure 3; Table 4), is consistent with the analyzed composite drill-hole sample (~15 kg), showing 75 ppb Pd at 0.5 wt.% Cu or 3300 ppb Pd (measured contents of Pd are normalized to 100% chalcopyrite or 33 wt.% Cu) [53].

The Vathi, Pontokerasia, Gerakario, and the Skouries porphyry deposits are all hosted in the Vertiskos Formation of SMM (Figure 1), but they display different geochemical data compared to the Skouries deposit, the Afton deposits, British Columbia, and other porphyry deposits (Table 5). The Vahti, Pontokerasia, Gerakario, as well as the porphyry-Cu deposits of Russia and Mongolia exhibit larger Mo, Ba, Zr, and U and smaller Cr, Ni, Mg, Pd, Pt, and Au contents (Table 5) [16–19,54–56].

Although an overlapping may occur in the plots of the Pd and Pt contents, versus the (Ba+Sr) and (Cr+Ni) contents, the smaller (Ba+Sr) content and the maximum contents of Mg, Cr, Ni, and Co seem to be characteristic of the precious metal fertile intrusions (Table 5; Figure 5).

Table 4. Major and trace element contents in the Skouries porphyry-Cu-Au-Pd-Pt samples from drill-holes of varying depths [present study] and Bulgaria [13].

		ppm															wt.%								ppb			
ID Sample	**Depth (m)**	**Mo**	**Pb**	**Zn**	**Ni**	**Co**	**Mn**	**Sr**	**V**	**La**	**Cr**	**Ba**	**W**	**Zr**	**Y**	**Cu**	**Fe**	**Al**	**Ti**	**Ca**	**Mg**	**K**	**Na**	**P**	**Pd**	**Pt**	**Au**	**Pd/Pt**
Greece																												
Skouries																												
SOP1	328	1.0	54	55	300	28	330	116	76	13	176	230	400	0.3	19	2.95	5.56	5.63	0.25	1.74	1.87	3.42	1.19	0.13	53	42	4800	1.3
SOP1	635	2.0	21	38	42	26	340	200	105	29	50	250	690	4.8	22	0.06	2.72	7.11	0.46	3.35	2.05	1.46	1.63	0.06	5.1	5	5	1.0
SOP1	636	8	15	32	71	21	210	125	100	28	59	200	350	2.7	22	0.07	2.81	6.63	0.46	1.25	2.02	1.65	1.35	0.06	3.2	5	50	0.6
SOP06	363	1.1	21	40	10	30	220	960	61	29	30	200	690	12	10	0.51	3.50	6.11	0.10	1.17	0.49	3.11	2.17	0.07	85	20	680	4.3
SOP06	365	1.6	75	51	19	29	270	330	74	6.6	21	960	590	5.8	3.2	2.13	8.01	4.11	0.08	0.50	0.49	3.30	0.95	0.03	50	49	3900	1.0
SOP06	525	1.2	45	110	370	71	785	150	110	53	275	44	420	5.3	29	0.94	7.34	6.14	0.27	4.50	3.00	0.52	1.50	0.07	6	5	120	1.2
SOP09	251	0.8	28	120	400	44	480	44	68	28	516	58	410	1.7	24	1.11	4.74	3.30	0.19	3.78	4.31	2.51	0.67	0.06	30	32	1400	0.9
SOP09	476	0.9	6	48	480	47	470	165	102	32	310	150	500	2.0	16	0.03	3.6	6.28	0.29	2.14	6.0	2.52	1.1	0.06	2	5	11	0.2
SOP18	142	2.5	105	53	48	25	190	462	32	18	14	1200	540	8.3	16	1.66	3.17	5.64	0.11	0.76	0.60	4.43	1.65	0.14	40	60	3800	0.7
SOP39	446	3.0	30	60	10	74	80	38	92	2.1	10	220	900	6.6	0.3	2.53	10.40	1.16	0.02	0.14	0.03	1.03	0.19	0.01	600	70	9600	8.7
SOP43	200	1.0	13	130	560	56	720	40	82	12	480	70	290	5.7	9.0	1.56	6.45	3.58	0.20	1.23	5.86	1.91	0.63	0.03	15	5	1500	3.0
SOP46	50	50	50	94	130	30	240	250	115	34	125	345	140	14.0	13	0.14	3.36	8.63	0.34	1.22	2.15	1.55	4.28	0.06	1	5	70	0.2
SOP76	170	100	12	180	500	40	370	50	110	47	690	220	90	6.0	11	0.7	5.03	5.94	0.31	0.74	6.92	2.53	0.49	0.03	2	5	600	0.4
SG-6	30	7.0	23	50	13	27	13	93	55	13	17	510	340	15	3.1	3.1	2.78	2.5	0.05	0.03	0.1	1.4	0.16	<0.01	360	31	3050	12
SG-6	110	2.0	71	66	17	62	150	640	51	24	6	1600	750	25	7.4	0.39	5.15	5.9	0.1	0.55	0.53	3.54	2.19	0.07	28	10	850	2.8
SG-6	465	1.0	31	46	7	41	70	22	70	2.5	7	120	460	4	<0.5	1.9	7.87	0.8	0.01	0.17	0.03	0.62	0.1	<0.01	410	26	5280	16
SG-6	494	1.0	21	60	10	43	57	43	76	2.9	17	310	440	8	<0.5	2.84	10.7	1.46	0.02	0.07	0.06	1.31	0.1	<0.01	420	150	12,900	2.8
SK8	130	1.0	23	53	21	48	138	55	61	2.8	8	330	530	9	<0.5	1.2	7.36	1.76	0.03	0.16	0.05	1.35	0.37	<0.01	20	5	1700	n.a.
SK8	390	82	71	180	13	70	56	58	33	13	10	270	830	5	1.8	3.2	6.1	1.0	0.02	0.04	0.08	0.7	0.27	<0.01	22	5	1600	n.a.
SK8	670	25	31	63	48	38	240	200	100	25	60	330	240	16	12	1.16	4.3	6.8	0.39	1.3	2.02	2.5	2.83	0.03	140	5	1580	n.a.
SK8	620	1	21	100	70	24	370	70	170	6.2	60	110	150	5.3	6.9	3.1	10.9	3.3	0.17	4.63	1.18	1.6	0.11	0.02	17	5	1520	n.a.
Average		14	37	78	150	42	276	196	83	20	140	370	460	7.7	12	7.13	5.8	4.5	0.18	1.56	1.9	2.1	1.14	0.06	110	31	2620	3.4
Bulgaria																												
Elatsite																												
PC-5		1	43	128	1	8	24	4	64	3.3	10	50	<10	7.7	0.6	12.8	14.2	0.6	0.01	0.03	0.44	0.27	0.02	0.01	6	20	100	0.3
PC-6		24.0	240	51	9	10	2670	250	67	26	25	130	120	9	22	0.06	5.04	1.4	0.02	15.3	0.6	0.64	0.06	0.08	10	8	39	1.3
Assarel																												
PC-2		3	52	38	8	12	41	35	63	18	14	440	12	20	3.6	0.98	4.4	6.53	0.04	0.15	0.23	1.35	0.2	0.02	5	1.2	250	4.2
Medet																												
PC-3		8	2	31	14	6	230	230	90	31	32	650	<10	22	13	0.17	2.31	7.04	0.28	0.86	1.34	3.3	2.5	0.05	10	19	12	0.8
PC-4		7	6	130	8	34	240	580	300	31	18	610	<10	15	16	2.71	5.03	6.9	0.23	1.74	1.42	3.5	1.7	0.17	50	26	340	1.9
Mo-Med		14,620	2	7	1	n.a.	24	60	n.a.	2.4	6	190	20	1.2	2.7	0.17	0.37	1.58	0.02	1.13	0.13	1.0	0.5	0.01	33	47	35	0.7
Tsar																												
Assen																												
PC-13		2	16	100	13	15	700	190	260	19	100	240	<10	50	54	1.31	9.37	7.1	0.42	1.12	2.4	1.2	1.47	0.07	49	51	95	1.0
PC-19		2	10	37	9	75	380	95	180	13	9	240	<10	18	7.4	0.36	4.7	4.34	0.1	1.95	0.35	3.1	0.22	0.09	130	21	200	0.7

Table 5. Mean values of selected trace elements taken into consideration to divide the PGE poor for the PGE fertile, in highly mineralized ore (Sf.C) and flotation concentrates (F.C) samples from porphyry-Cu deposits; n.d. = not detected; n.a. = not available.

			wt.%			ppb					ppm								
Country	**Deposit**	**Description**	**Mg**	**Cu**	**Cu/Mo**	**Au**	**Pt**	**Pd**	**Pd/Pt**	**Ni**	**Cr**	**Sr**	**Ba**	**Y**	**Zr**	**Th**	**U**	**Th/U**	**Reference**
PGE-poor porphyry-Cu-Mo deposits																			
Chalkidiki Peninsula	Vathi	Sf.C	0.43	0.3	50	526	10	3	0.3	14	30	138	780	20	86	42	31	1.4	[36]
	Gerakario	Sf.C	0.7	1.92	190	535	10	3.2	0.32	13	21	140	1440	55	160	15	4.0	3.8	[54]
	Pontokerasia	Sf.C	0.5	1.38	120	59	10	1.3	0.13	15	13	300	1160	63	175	35	22	1.6	[54]
Russia	Sora	Sf.C	0.18	0.05	8.6	17	<10	13	n.a.	4	21	280	1150	7.7	120	5.8	2.5	2.3	Present study; [55]
	Aksug	Sf.C	0.36	0.15	0.17	64	18	20	0.9	3.4	21	310	760	3.3	34	1.4	1.1	1.3	
	Zhireken	Sf.C	0.20	0.02	1.4	33	16	28	0.62	5.6	32	250	670	4.2	55	7.5	4.5	1.7	
Mongolia	Erdentetuin-Obo	Sf.C	0.37	0.15	0.92	21	14	22	0.71	11	30	540	1250	4.6	51	3.2	1.0	3.2	Present study; [55]
PGE-fertile porphyry-Cu-Au deposits																			
Greece	Skouries	Sf.C	2.8	1.28	985	2790	29	125	4.31	120	210	230	390	14	6.3	30	5.6	5.3	Present study; [13].
	Skouries	F.C	n.a.	21	10,500	22,000	40	2400	60	90	20	n.a.	n.a.	n.a.	n.a.	n.a.	n.a.	n.a.	[13]
Bulgaria	Elatsite	Sf.C	1.6	9.7	3060	3600	28	220	7.9	10	94	150	640	16	86	6.3	4.5	1.4	[13,16,17,19,56,57]
	Elatsite	Sf.C	n.a.	45.3	n.a.	1100	900	4500	5.0	n.a.	3	n.a.	n.a.	n.a.	n.a.	n.a.	n.a.	n.a.	[13]
	Tsar Assen	Sf.C	1.4	0.84	4200	150	36	90	2.5	11	55	140	240	30	34	n.a.	n.a.	n.a.	
Serbia	Veliki Kjagra	F.C	n.a.		110	4625	16	70	4.4	n.a.	n.a.	n.a.	n.a.	n.a.	n.a.	n.a.	n.a.	n.a.	[15,20]
	Majdanpek	F.C	n.a.	26	120	4600	40	180	4.5	n.a.	n.a.	n.a.	n.a.	n.a.	n.a.	n.a.	n.a.	n.a.	[15]
	Bor	F.C	n.a.	n.a.	n.a.	1700	19	40	2.1	n.a.	n.a.	n.a.	n.a.	n.a.	n.a.	n.a.	n.a.	n.a.	
Philippines	Santo Tomas II	Sf.C	n.a.	0.7	n.a.	3500	10	67	6.7	n.a.	n.a.	n.a.	n.a.	n.a.	n.a.	n.a.	n.a.	n.a.	[15]
	Biga	F.C	n.a.	n.a.		2350	8	56	7.0	n.a.	n.a.	n.a.	n.a.	n.a.	n.a.	n.a.	n.a.	n.a.	
Malaysia	Mamut	F.C	n.a.	20.4	n.a.	15,300	470	1400	2.6	n.a.	n.a.	n.a.	n.a.	n.a.	n.a.	n.a.	n.a.	n.a.	[15]
Papua New Guinea	Ok Tedi	F.C	n.a.	31.9	n.a.	28,000	24	880	36.7	n.a.	n.a.	n.a.	n.a.	n.a.	n.a.	n.a.	n.a.	n.a.	[15,20]
	Panguna	F.C	n.a.	21.4	93	1035	8	40	5.8	n.a.	n.a.	n.a.	n.a.	n.a.	n.a.	n.a.	n.a.	n.a.	[20]
Indonesia	Grasberg	F.C	n.a.	23.8	n.a.	18,000	15	58	3.9	n.a.	n.a.	n.a.	n.a.	n.a.	n.a.	n.a.	n.a.	n.a.	[15]
British Columbia, Cordillera	Galore Creek	Sf.C	n.a.	15.1	n.a.	34,200	48	780	15.2	n.a.	n.a.	n.a.	n.a.	n.a.	n.a.	n.a.	n.a.	n.a.	[19]
	Mt. Polley	Sf.C	n.a.	20.6	n.a.	23,600	32	320	10	n.a.	n.a.	n.a.	n.a.	n.a.	n.a.	n.a.	n.a.	n.a.	
	Mt. Milligan	Sf.C	n.a.	6.8	n.a.	18,500	110	6300	57.3	n.a.	n.a.	n.a.	n.a.	n.a.	n.a.	n.a.	n.a.	n.a.	
	Ajax	Sf.C	n.a.	26.3	n.a.	990	8	140	17.5	n.a.	n.a.	n.a.	n.a.	n.a.	n.a.	n.a.	n.a.	n.a.	
	Afton	Sf.C	2.2	3.8	4447	4094	34	760	22.4	144	96	60	84	n.a.	n.a.	0.74	0.4	1.8	
	Allard, La plata	Sf.C	n.a.	18	n.a.	1230	2880	1920	0.7	n.a.	n.a.	n.a.	n.a.	n.a.	n.a.	n.a.	n.a.	n.a.	
	Allard, La plata	F.C	n.a.	27	n.a.	1740	3935	2320	0.6	n.a.	n.a.	n.a.	n.a.	n.a.	n.a.	n.a.	n.a.	n.a.	
	Copper King Mine	F.C	n.a.	31.5	n.a.	440	900	2660	3	n.a.	n.a.	n.a.	n.a.	n.a.	n.a.	n.a.	n.a.	n.a.	
	Copper King Mine	Sf.C	n.a.	22	n.a.	190	13,600	6430	0.5	n.a.	n.a.	n.a.	n.a.	n.a.	n.a.	n.a.	n.a.	n.a.	
	Cooper Mountain	F.C	n.a.	28.2	n.a.	4800	190	2760	14.5	n.a.	n.a.	n.a.	n.a.	n.a.	n.a.	n.a.	n.a.	n.a.	
	Cooper Mountain	Sf.C	n.a.	40	n.a.	4200	50	3250	65	n.a.	n.a.	n.a.	n.a.	n.a.	n.a.	n.a.	n.a.	n.a.	

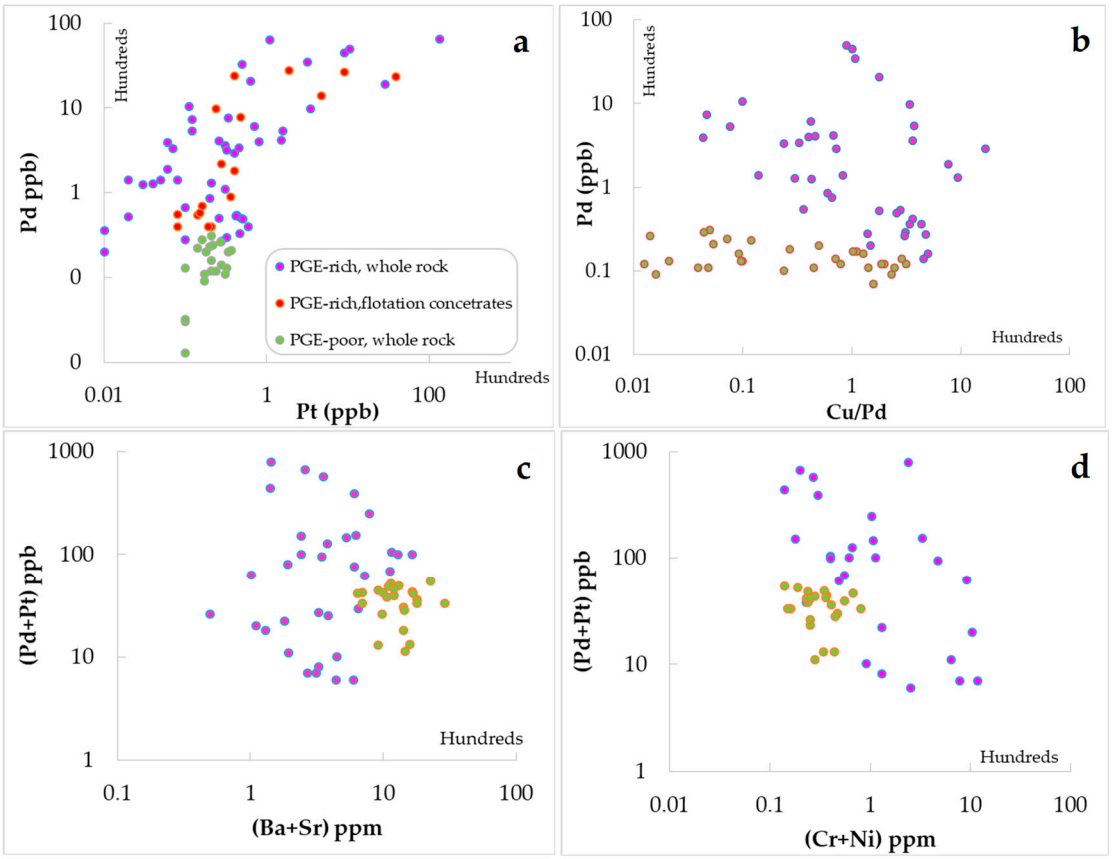

Figure 5. (**a**): Plots of the Pd versus Pt content for whole rock and flotation concentrates: (**b**): plot of Pd versus Cu/Pd); (**c**,**d**): plots of the (Pd+Pt) content versus (Ba+Sr) and (Cr+Ni) contents for PGE-rich and PGE-poor, whole rock analyses. Data from Tables 3 and 4, and [13,22,58]. PGE-rich and PGE-poor in the Figure 5b–d are presented as in Figure 5a.

4. Discussion

The review of our data and those available in the literature allow us to distinguish a PGE-poor group and a PGE-rich group of porphyry-Cu deposits. In particular, in the Vathi, Pontokerasia, Gerakario deposits (Greece) and those from Russia, the whole rock (Pd+Pt) content is very low, being between 11 and 44 ppb. The PGE-fertile group comprises examples from Skouries (Greece), Bulgaria, Serbia, the Philippines, Malaysia, Papua New Guinea, British Columbia, and Cordillera and are characterized by a significant difference in the (Pd+Pt) content, with values of (Pd+Pt) comprised between 48 and 6255 ppb in flotation concentrates and 126 and 6410 ppm in whole rock analyses (Table 5). An exceptionally high whole rock content of (Pd+Pt), up to 20,030, has been reported in one sample analyzed in the Copper King Mine of Cordillera (Table 5).

In order to better understand how the relative enrichment in Pt and Pd was achieved only in few porphyry-Cu deposits, the following factors are discussed in detail:

(1) Sources of precious metals in porphyry-Cu deposits;
(2) Transport of PGE in hydrothermal systems,
(3) Genetic significance of the oxidized nature of parent magmas;
(4) Fertility of porphyry-Cu deposits.

4.1. Sources of Precious Metals in Porphyry-Cu Deposits

Potential source regions of lithospheric re-fertilization include subduction-modified lower crust, sub-continental lithospheric mantle, or lower crust formed by under plated arc mafic rocks [7,43,59–65]. Melting the mantle at oxidizing conditions destabilizes and removes sulfide phases, while the coexisting melt may be enriched in precious metals

(Pt, Pd, and Au) relative to their primitive mantle values [66–81]. The presence of mafic (gabbroic) rocks fined-grained "basaltoid" dykes are known in the environment of Elatsite porphyry mineralization [17,67–70]. Also, detailed field studies in the Valerianov–Beltau–Kurama magmatic arc, Uzbekistan, revealed the occurrence of gabbroic intrusions at depth and along the periphery of the ore field, and have established their spatio-temporal relationship with fertile porphyries [71,72]. In addition, the formation of melts more favorable for generating porphyry Au-Cu deposits has been attributed to several processes, such as slab rollback caused asthenospheric mantle upwelling, the melting of metabasaltic amphibolites that underplated subducted continental crust, and shoshonitic lower Miocene magmatic rocks on Skouries (Chalkidiki) [73–77]. Ophiolites and associated ore deposits (mainly chromitites) in the SMM (Figure 1) [82–84] may have been affected during their multistage evolution by several processes in the mantle wedge above a subduction zone and crust, such as partial melting, fractional crystallization, interactions between mantle and lithospheric slab, and metal recycling [85–88]. During the progressively collisional subduction of Tethys [26], an interaction between a varying degree of mantle-derived magma with the crust and the genesis of magma rich in water and sulfur with a significant mafic contribution to the magma source may have played an important role in the fertility of the Skouries porphyry-Cu deposit. Therefore, we can argue that an influx of a PGE-rich mafic magma related with the complex processes occurring in the supra-subduction zone was probably responsible for the original enrichment of Pd and Pt in certain porphyry-Cu deposits, as illustrated in Figure 6.

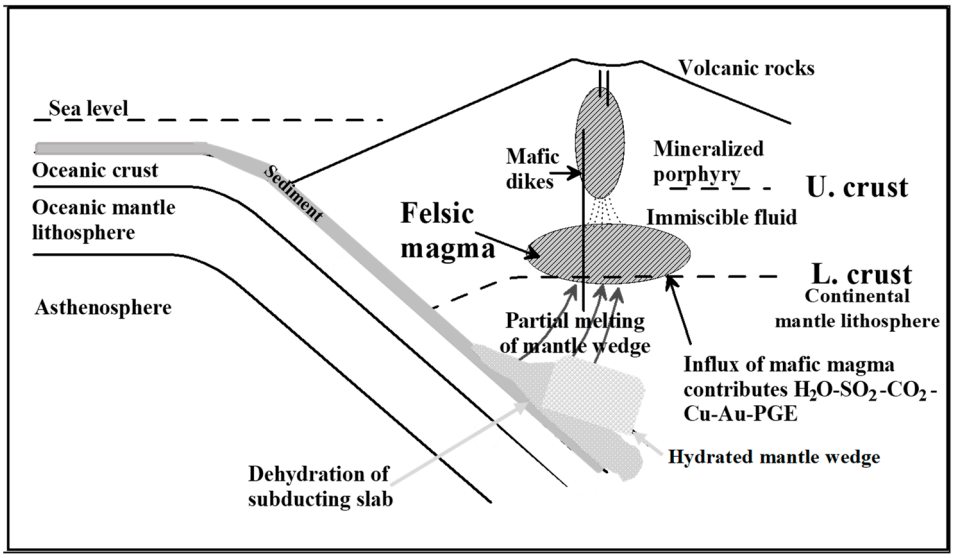

Figure 6. Schematic section of a subduction zone and continental arc, showing the geotectonic setting for porphyry-Cu-Au-Pd±Pt systems. Partial melting of metasomatized mantle generates mafic melts, which may contribute metals, including PGE and sulfur, potentially incorporated into the overlying felsic magma chamber. Hydrous, metal-bearing extracted from the subducting slab rising into the mantle wedge may cause metasomatism [78–81].

The larger Mg, Cr, Ni, Co, Re, and ^{187}Os contents and smaller LILE elements (Ba and Sr) in fertile porphyry-Cu-Au- (PGE) reflect the larger contribution made by the mantle to the parent magmas [67–70]. In contrast, the smaller Mg, Cr, Ni, Co, and Re contents and larger Ba and Sr in PGE-poor porphyry-Cu-Mo deposits from the Chalkidiki Peninsula (Vathi, Pontokerasia and Gerakario) and Russia suggest the presence of parent magmas with a more crustal contribution [76,77]. Although the overlapping in relevant plots (Figure 5) is not precluded, it is obvious that in selected plots (Figure 5), two populations can be distinguished, the PGE-enriched and PGE-poor porphyry-Cu deposits. In addition, there is not any distinction between the PGE-rich whole rock analyses and those of PGE-rich flotation concentrates.

Chondrite-normalized REE patterns, specifically highly fractionated LREE (Figure 3; [42] and elevated incompatible LILE, including Sr and Ba (Tables 2 and 3), suggest the involvement of subduction-enriched continental lithosphere, while the minor Eu/Eu* anomaly (Figure 4) and abundant amphibole and biotite may indicate elevated magmatic water [42,74,75].

4.2. Transport of PGE in Hydrothermal Systems

Merenskyite (the most common PGE-mineral) occurs commonly as inclusions or on the edge of hydrothermal chalcopyrite [18,19,37], suggesting that their crystallization was related with the presence of hydrothermal fluids [63]. The current state of knowledge of the solubility of PGE has been reviewed and applied in hydrothermal systems [63–65]. Recent experimental data have shown that the solubility of Au and Pd both have positive relationships with fO_2, temperature, acidity, and total chloride concentration (Cltotal), while Pt is efficiently mobilized at magmatic temperatures in relatively oxidized, slightly acidic, high-salinity brines [65]. According to these authors, calculated fluid/melt partition coefficients for Au and Pd in low-density magmatic vapors suggest that Pd may experience decoupling from Au in porphyry Au-Cu (±Pd, Pt) systems due to the restricted compatibility of Pd in the fluid phase (requiring strongly acidic and substantially high fO_2 conditions). Also, the main mechanisms that promote the deposition of Pt from high-temperature aqueous brines are a reduction in fO_2, temperature, acidity, and the total chloride concentration. Therefore, we suggest that local and randomly distributed enrichment in Pt and Pd in some porphyry Au-Cu (±Pd, Pt) deposits may have been caused by the circulation of complex hydrothermal fluids.

4.3. Genetic Significance of the Oxidized Nature of Parent Magmas

The incorporation into the melt of precious metal-bearing Fe-Ni-Cu-sulfides, hosted in mantle-derived rocks, may be an important step in the genesis of those deposits, because the magmatic sulfide melts can act as intermediate Cu and precious metals hosts during the evolution of the magmatic system [89–91]. It has been established that the oxidized nature of parent magma is connected with the ability to produce a magmatic–hydrothermal system with ideal chemistry that facilitates the capacity for transporting sufficient precious metals [73,89]. Specifically, the oxidized nature of the alkaline arc magmas inhibits PGE to precipitate as sulfides, allowing the Pd and Pt to remain in the magmas, and thus they can be transported by magmatic–hydrothermal fluids and precipitated in the porphyry environment [59]. Since hydrothermal magnetite associated with chalcopyrite and bornite in porphyry systems is favored at high temperatures and fO_2, and low fS_2 [91], the occurrence of abundant (average 6 vol.%) magnetite (reaching up to 10 vol.%) in the Skouries deposit, that is linked to pervasive potassic and propylitic alteration type [19], is considered to be a characteristic feature of the oxidation state of Pd-bearing porphyry Cu deposits. In contrast, "reduced" porphyry Cu-Au deposits, lacking primary magnetite and sulfate minerals (anhydrite), contain abundant pyrrhotite and are relatively Cu-poor, but they are Au-rich [59,92,93].

Dilles et al. [94] investigated porphyry Cu (±Mo±Au) and epithermal Au-Ag deposits formed by magmatic–hydrothermal fluids in Phanerozoic convergent margin settings and reported SHRIMP-RG ion microprobe analyses of Hf, Ti, and REE abundances in zircon. These authors compared the compositions of zircons generally in fertile and barren granitic plutons, and observed an Eu/Eu* ratio higher than 0.4 only in zircons associated with fertile granites, thus concluding that zircon composition is potentially a valuable tool for mineral exploration [94]. Similar analytical data on the zircons from the Skouries mineralized porphyry are not available. Tiny zircon crystals occurring as inclusions and/or at the peripheral parts of magnetite are common in the Skouries deposit (Figure 3c,d), suggesting a genetic link between zircon and magnetite. The bulk rock analysis on magnetite separates from the Skouries deposit indicated values for the Eu/Eu* ratio higher than 0.35, ranging from 0.55 to 1.7 (Table 4). Although the presence of magnetite is considered to

be a characteristic feature of the oxidation state of porphyry Cu deposits [19,59,92], the above-reported Eu/Eu* ratios in the magnetite separates are consistent with a relatively high oxidation state during the cooling of the ore-forming system, which permitted the transportation of Pd and Pt in the magmatic–hydrothermal system.

4.4. Fertility of Porphyry-Cu Deposits

The mantle source that underwent a partial melting of existing sulfides is a critical control of the PGE contents in the resulting melts. Therefore, the predominant factors controlling the distribution of PGE are the partial melting of the mantle source, the interaction of the magmas with magmatic sulfide liquids, the partition coefficients of PGE from silicate into sulfide liquids being of the order of thousands, and the Pd solubility in silicate melts orders of magnitude higher than that of other PGE [7]. In some cases, the formation of an immiscible sulfide liquid enriched in the more chalcophile PPGE (Pt, Pd, and Rh sub-group) can be achieved in certain magmas during their cooling, giving rise to the precipitation of PPGE minerals together with Ni-Cu-Fe sulfides, as interstitial in chromite ores and cumulus silicates [6,94].

However, the fertility of the porphyry Cu-Au-Pd-Pt deposits and the mechanism permitting the transfer of these elements from the mantle to the magma source for porphyry–epithermal deposits still remain unclear [22,24,25]. The available texture intergrowths, mineral chemistry, and geochemical data (Figure 3; Tables 2–5) are consistent with the significant role of the critical degree of mantle melting to release Pt and Pd in the ore-forming fluids, the high oxidation state, high magmatic water content, and the degree of fractionation. The larger Mg, Cr, Ni, and Co contents in bulk rock analyses, in the mineral chemistry (sulfides and magnetite), and smaller Sr and Ba (LILE elements) contents in fertile porphyry-Cu deposits from the Balkan Peninsula and British Columbia, in contrast to those from the Vathi, Pontokerasia, Gerakario, Russia, and Mongolia deposits (Tables 2–5; Figure 5), indicate that the composition of the parent magma is mainly affected from a mantle component rather that lower crust. The investigation of the characteristic features of porphyry-Cu-Au-Pd±Pt intrusions, such as the Elatsite, has shown that mantle-derived methane was identified in two-phase (CO_2-CH_4) high-temperature (>500 °C) fluid inclusions [68]. That type of fluid inclusion may suggest that carbon, as a supercritical CO_2 fluid, could be present in the primitive Elatsite magmas, promoting the physical transport of sulfides and/or telluride melt droplets [18,94]. It has been noted that a small amount of reduced gases in fluid inclusions cannot argue against the oxidized feature of the magmas during the final mineralization process of porphyry deposits [92]. Although most of the hydrogen and methane should have been oxidized by ferric Fe, some of the reduced gases may be trapped in fluid inclusions [92].

Also, detailed Pb, Sr, S, O, and C isotopic data have been applied on the porpyry Cu deposits of the Chalkidiki Peninsula [34]. These Tertiary intrusions are characterized by a rather diffuse Sr isotopic pattern, suggesting heterogeneous crustal rocks (meta-igneous and metasedimentary), while relatively low initial Sr values (<~0.707) indicated either a mantle component and/or a component from lower crustal rocks [34]. Also, the Pb isotope composition outlined by whole rock, feldspar, and ore minerals from Skouries suggests a major contribution of country rocks from the Vertiskos Formation at depths prior to the final emplacement [34]. Bonev et al. [95] have reported on the isotopic compositions of metamafic rocks exposed in the SMM, consisting of high- and low-Ti gabbroic and basaltic rocks, showing Nd-Sr-Pb isotope signatures compatible with mantle-derived MORB (Mid-Ocean Ridge Basalts) and OIB (Ocean Island Basalts) components with a small amount of crustal material involved in their melt source. These authors suggested that such isotopic features, coupled with field observations, reflect an intra-continental rift origin of those metamafic rocks protolith [95].

In addition to the contribution by mantle-derived components, the fractionation degree of the mineralized system seems to be of particular importance too. The Pd/Pt ratio, that may reflect the degree of fractionation in the ore-forming system (due to the

higher solubility of Pd compared to Pt), ranges from 0.6 to 0.9 in the PGE-poor porphyry deposits of Russia and Mongolia, and 0.13 to 0.9 in the Vathi, Pontokerasia, and Gerakatio PGE-poor deposits, in contrast to the (Pd, Pt, Au)-fertile deposits in Skouries (average 4.3 up to 60), Elatsite (average 7.8), and British Columbia (average 19) (Table 5). The variation in the Pd/Pt ratio may reflect differences in their evolution systems. Tetrahedrite–tennantite are frequently associated with the magnetite–bornite–chalcopyrite assemblage of an early stage of mineralization in porphyry deposits, which are in a spatial association with epithermal deposits. Some examples include the Elatsite deposit associated with the Chelopech Au-Cu high-sulfidation epithermal deposit, the Assarel deposits in Bulgaria, and the Bor/Majdanpek porphyry deposits in Serbia and in British Columbia, although they are rare in the Skouries deposit [21,68,69,96,97]. Thus, a higher degree of fractionation for the fertile porphyry-Cu-Au-Pd±Pt-forming system compared to porphyry Cu-Mo deposits is consistent with the often proximity and overlapping of the former with epithermal-type deposits [24,26,68,69]. Similarly, the presence of zircons having low Th/U and high Yb/Gd associated with the mineralized phases ratios in porphyry-fertile Late Triassic and Early Jurassic plutons in British Columbia suggests their precipitation after fractional crystallization to some extent [24]. The elevated values of the Pd/Pt ratios, the extremely low Cr contents (<1 ppm) in high Cu-Pd-Pt-grade ores, and a negative correlation between Cr content and the Pd/Pt values in porphyry deposits of the Balkan Peninsula [13] suggest a genesis from more evolved mineralized fluids in porphyry Cu-Au-Pd-Pt deposits. The significant role of the crystal fractionation process that led to the formation of immiscible sulfide enriched in PPGE (Pt, Pd and Rh sub-group), giving rise to the precipitation of PPGE minerals together with Ni-Cu-Fe sulfides, as interstitial in chromite ores and cumulus silicates, has been emphasized [6,52].

5. Conclusions—Implications for Mineral Exploration

The presented mineral chemistry and geochemical data on selected porphyry-Cu deposits distributed worldwide, coupled with petrological evidence, may allow to define significant differences between PGE-fertile and PGE-poor porphyry-Cu intrusions, especially in the deposits of Balkan Peninsula, Russia, and Mongolia.

- Critical factors controlling the PGE-fertility of porphyry-Cu systems may be the spatial and temporal relationship of mafic (gabbroic) rocks with porphyries (for example, in the Elatsite deposit), which is reflected in the composition of the magma, and the favorable conditions for the transfer of metals from the magma to the fluids and fertile porphyry-Cu deposits.
- Fertile porphyry Cu+Au+Pd±Pt deposits from the Balkan Peninsula are characterized by larger Mg, Cr, Ni, and Re contents and smaller Ba and Sr (LILE elements) compared to PGE-poor porphyry-Cu-Mo from Russia, Mongolia, and Vathi–Pontokerasia–Gerakario deposits.
- The common presence of high PGE mineralization [thousands ppb (Pd+Pt)] and low Cr content in the transition from the porphyry to epithermal environment, coupled with the occurrence of Pd-, Te-, and Se-bearing minerals (merenskyite, clausthalite) and tetrahedrite–tennantite in fertile porphyry Cu deposits (Elatsite deposit), reflect a highly fractionated ore-forming system.
- The occurrence of abundant Cr-bearing magnetite, abundant amphibole and biotite (abundant magmatic water), high Mg, Cr, Ni, and Re contents, and low Ba and Sr in bulk rock analyses is considered to be encouraging evidence for finding PGE-rich Cu+Au+Pd±Pt deposits in the future.

Author Contributions: Conceptualization and methodology: M.E.-E., F.Z. and G.G.; software and validation of data: M.E.-E.; writing—original draft preparation: M.E.-E., F.Z. and G.G. All authors have read and agreed to the published version of the manuscript.

Funding: This research received no external funding.

Data Availability Statement: All papers are presented in this article.

Acknowledgments: Many thanks are expressed to the reviewers and Editors for their constructive criticism, the University of Athens, and all the cited authors providing valuable literature data on the topic of this review.

Conflicts of Interest: The authors declare no conflict of interest.

References

1. Anderson, P. Chinese assessments of "critical" and "strategic" raw materials: Concepts, categories, policies, and implications. *Extr. Ind. Soc.* **2020**, *7*, 127–137. [CrossRef]
2. Zhou, L.; Fan, H.; Ulrich, T. Editorial for Special Issue "Critical Metals in Hydrothermal Ores: Resources, Recovery, and Challenges. *Minerals* **2021**, *11*, 299. [CrossRef]
3. Naldrett, A.J.; Von Gruenevaldt, G. The association of PGE with chromitite in layered intrusions and ophiolite complexes. *Econ. Geol.* **1989**, *84*, 180–187. [CrossRef]
4. Cawthorn, R.G. The Platinum Group Element Deposits of the Bushveld Complex in South Africa. *Platin. Met. Rev.* **2010**, *54*, 205–215. [CrossRef]
5. Eliopoulos, I.-P.; Eliopoulos, G.; Sfendoni, T.; Economou-Eliopoulos, M. Cycling of Pt, Pd, and Rh Derived from Catalytic Converters: Potential Pathways and Biogeochemical Processes. *Minerals* **2022**, *12*, 917. [CrossRef]
6. Zaccarini, F.; Economou-Eliopoulos, M.; Kiseleva, O.; Garuti, G.; Tsikouras, V. Platinum Group Elements (PGE) Geochemistry and Mineralogy of Low Economic Potential (Rh-Pt-Pd)-Rich Chromitites from Ophiolite Complexes. *Minerals* **2022**, *12*, 1565. [CrossRef]
7. Barnes, S.J.; Mungall, J.E.; Maier, W.D. Platinum group elements in mantle melts and mantle samples. *Lithos* **2015**, *232*, 395–417. [CrossRef]
8. Werle, J.I.; Ikramuddin, M.; Mutschler, F.E. Allard stock, La Plata Mountains, Colorado—An alkaline rock hosted porphyry copper precious metal deposit. *Can. J. Earth Sci.* **1984**, *21*, 630–641. [CrossRef]
9. Mutschler, F.E.; Griffin, M.E.; Scott, S.D.; Shannon, S.S. Precious metal deposits related to alkaline rocks in the north American Cordillera—An interpretive review. *Geol. Soc. S. Afr. Trans.* **1984**, *88*, 355–377.
10. Tarkian, M.; Koopmann, G. Platinum-group minerals in the Santo Tomas II Philex porphyry copper–gold deposit, Luzon Island, Philippines. *Miner. Depos.* **1995**, *30*, 39–47. [CrossRef]
11. Eliopoulos, D.G.; Economou-Eliopoulos, M. Platinum-Group Element and Gold Contents in the Skouries Porphyry-Copper deposit, Chalkidiki Peninsula, Northern Greece. *Econ. Geol.* **1991**, *86*, 740–749. [CrossRef]
12. Eliopoulos, D.G.; Economou-Eliopoulos, M.; Strashimirov, S.; Kovachev, V.; Zhelyaskova-Panayotova, M. Gold, platinum and palladium content in porphyry Cu deposits from Bulgaria: A study in progress. *Geol. Soc. Greece* **1995**, *5*, 712–716.
13. Eliopoulos, D.G.; Economou-Eliopoulos, M.; Zhelyaskova-Panayiotova, M. Critical factors controlling Pd and Pt potential in porphyry Cu-Au deposits: Evidence from the Balkan Peninsula. *Geosciences* **2014**, *4*, 31–49. [CrossRef]
14. Pašava, J.; Vymazalová, A.; Košler, J.; Koneev, R.I.; Jukov, A.V.; Khalmatov, R.A. Platinum-group elements in ores from the Kalmakyr. Porphyry Cu–Au–Mo deposit, Uzbekistan: Bulk geochemical and laser ablation ICP-MS data. *Miner. Depos.* **2010**, *45*, 411–418. [CrossRef]
15. Tarkian, M.; Stribrny, B. Platinum-group elements in porphyry copper deposits: A reconnaissance study. *Mineral. Petrol.* **1999**, *65*, 161–183. [CrossRef]
16. Tarkian, M.; Hunken, U.; Tokmakchieva, M.; Bogdanov, K. Precious-metal distribution and fluid-inclusion petrography of the Elatsite porphyry copper deposit, Bulgaria. *Miner. Depos.* **2003**, *38*, 261–281. [CrossRef]
17. Augé, T.; Petrunov, R.; Bailly, L. On the mineralization of the PGE mineralization in the Elastite porphyry Cu–Au deposit, Bulgaria: Comparison with the Baula-Nuasahi Complex, India, and other alkaline PGE-rich porphyries. *Can. Mineral.* **2005**, *43*, 1355–1372. [CrossRef]
18. McFall, K.; McDonald, I.; Wilkinson, J.J. Assessing the Role of Tectono-Magmatic Setting in the Precious Metal (Au, Ag, PGE) and Critical Metal (Te, Se, Bi) Endowment of Porphyry Cu Deposits. *SEG Spec. Publ.* **2018**, *2*, 277–295.
19. Economou-Eliopoulos, M. Platinum-Group Element Potential of Porphyry Deposits. In *Mineralogical Association of Canada Short Course 35*; Mineralogical Association of Canada: Quebec, QC, Canada, 2005; pp. 203–245.
20. John, D.A.; Taylor, R.D. By-Products of Porphyry Copper and molybdenum Deposits. *Rev. Econ. Geol.* **2016**, *18*, 137–164.
21. Jankoviv, S. Ore-Deposit Types and Major Copper Metallogenic Units in Europe. European Copper Deposits, UNESCO-IGCP Projects 169 and 60; 1980. Volume 1, pp. 9–25. Available online: https://pascal-francis.inist.fr/vibad/index.php?action=getRecordDetail&idt=PASCALGEODEBRGM8120418504 (accessed on 9 August 2023).
22. Robb, S. Distribution of Platinum Group Elements in the New Afton Alkalic Cu-Au Porphyry Deposit, Kamloops, British Columbia. Master's Thesis, Carleton University, Ottava, ON, Canada, 2020; p. 130.
23. Kelley, K.D.; Ludington, S. Cripple Creek and other alkaline-related gold deposits in the southern Rocky Mountains, USA: Influence of regional tectonics. *Miner. Depos.* **2002**, *37*, 38–60. [CrossRef]
24. Bouzari, F.; Hart, C.J.R.; Bissig, T. Assessing British Columbia Porphyry Fertility in British Columbia Batholiths using Zircons. *Geosci. BC Rep.* **2020**, *450*, 24.

25. Holwell, D.A.; Fiorentini, M.L.; Knott, T.R.; McDonald, I.; Blanks, D.E.; McCuaig, C.; Gorczyk, W. Mobilisation of deep crustal sulfide melts as a first order control on upper lithospheric metallogeny. *Nat. Commun.* **2023**, *13*, 573. [CrossRef]
26. Voudouris, P.; Melfos, V.; Spy, P.G.; Bindi, L.; Kartal, T.; Arikas, K.; Moritz, R.; Ortelli, M. Rhenium-rich molybdenite and rheniite in the Pagoni Rachi Mo–Cu–Te–Ag–Au prospect, northern Greece: Implications for the re geochemistry of porphyry-style Cu–Mo and Mo mineralization. *Can. Mineral.* **2009**, *47*, 1013–1036. [CrossRef]
27. Arvanitidis, N.D. New metallogenetic concepts and substainability perspectives for non-energy metallic minerals in Central Macedonia, Greece. *Bull. Geol. Soc. Greece* **2010**, *43*, 2437–2445. [CrossRef]
28. Dixon, J.E.; Dimitriadis, S. Metamorphosed ophiolitic rocks from the Serbo-Macedonian Massif, near lake Volvi, North-east Greece. *Geol. Soc. Lond. Spec. Publ.* **1984**, *17*, 603–618. [CrossRef]
29. Tobey, E.; Schneider, A.; Alegria, A.; Olcay, L.; Perantonis, G.; Quiroga, J. Skouries Porphyry Copper/Gold Deposit, Chalkidiki, Greece. In *Porphyry Hydrothermal Cu–Au Deposits*; Porter, T.M., Ed.; PGC Publishing: Adelaide, Australia, 1998; pp. 159–168.
30. Piippo, S.; Sadeghi, M.; Koivisto, E.; Skyttä, P.; Baker, T. Semi-automated geological mapping and target generation from geochemical and magnetic data in Halkidiki region, Greece. *Ore Geol. Rev.* **2022**, *142*, 104714. [CrossRef]
31. Melfos, V.; Voudouris, P. Geological, Mineralogical and Geochemical Aspects for Critical and Rare Metals in Greece. *Minerals* **2012**, *2*, 300–317. [CrossRef]
32. Kockel, F.; Mollat, H.; Walther, H. *Erlanterungan zur Geologischen Karte der Chalkidiki und Angrenzender Gebiete*; Nord Griecheland: Hannover, Germany, 1977. (In German)
33. Perantonis, G. Genesis of Porphyry Copper Deposits in Chalkidiki Peninsula and W. Thrace, Greece. Ph.D. Thesis, University of Athens, Athens, Greece, 17 June 1982.
34. Frei, R. Isotope (Pb, Rb-Sr, S, O, C, U-Pb) Geochemical Investigations on Tertiary Intrusives and Related Mineralizations in the Serbomacedonian Pb-Zn, Sb+Cu-Mo Metallogenic Province in Northern Greece. Ph.D. Thesis, Swiss Federal Institute of Technology (ETH) Zurich, Zurich, Switzerland, 1993.
35. Bussolesi, M.; Grieco, G.; Zaccarini, F.; Cavallo, A.; Tzamos, E.; Storni, N. Chromite compositional variability and associated PGE enrichments in chromitites from the Gomati and Nea Roda ophiolite, Chalkidiki, Northern Greece. *Miner. Depos.* **2022**, *57*, 1323–1342. [CrossRef]
36. Stergiou, C.L.; Melfos, V.; Voudouris, P.; Spry, P.G.; Papadopoulou, L.; Chatzipetros, A.; Giouri, K.; Mavrogonatos, C.; Filippidis, A. The Geology, Geochemistry, and Origin of the Porphyry Cu-Au-(Mo) System at Vathi, Serbo-Macedonian Massif, Greece. *Appl. Sci.* **2021**, *11*, 479. [CrossRef]
37. Stergiou, C.L.; Melfos, V.; Voudouris, P.; Papadopoulou, L.; Spry, P.G.; Peytcheva, I.; Dimitrova, D.; Stefanova, E.; Giouri, K. Rare and Critical Metals in Pyrite, Chalcopyrite, Magnetite, and Titanite from the Vathi Porphyry Cu-Au±Mo Deposit, Northern Greece. *Minerals* **2021**, *11*, 630. [CrossRef]
38. Kroll, T.; Müller, D.; Seifert, T.; Herzig, P.M.; Schneider, A. Petrology and geochemistry of the shoshonite-hosted Skouries porphyry Cu–Au deposit, Chalkidiki, Greece. *Miner. Depos.* **2002**, *37*, 137–144. [CrossRef]
39. Tarkian, M.; Eliopoulos, D.G.; Economou-Eliopoulos, M. Mineralogy of precious metals in the Skouries porphyry copper deposit, Northern Greece. *Neues Jahrb. Mineral. Abh.* **1991**, *12*, 529–537.
40. Strasimirov, S.; Kovachev, V. Temperatures and ore formation in Cu-deposits from Srednogorie zone, based on fluid inclusion studies of minerals. *Rev. Bulg. Geol. Soc.* **1982**, *LIII 2*, 1–12.
41. Mavrogonatos, C.; Voudouris, P.; Berndt, J.; Klemme, S.; Zaccarini, F.; Spry, P.G.; Melfos, V.; Tarantola, A.; Keith, M.; Klemd, R.; et al. Trace Elements in Magnetite from the Pagoni Rachi Porphyry Prospect, NE Greece: Implications for Ore Genesis and Exploration. *Minerals* **2019**, *9*, 725. [CrossRef]
42. Siron, C.R.; Thompson, J.H.F.; Baker, T.; Friedman, R.; Tsitsanis, P.; Russell, S.; Randall, S.; Mortensen, J. Magmatic and metallogenic framework of Au-Cu porphyry and polymetallic carbonate-hosted replacement deposits of the Kassandra mining district, Northern Greece. *Soc. Econ. Geol. Spec. Publ.* **2016**, *19*, 29–55.
43. Taylor, S.R.; McLennan, S.M. *The Continental Crust: Its Composition and Evolution*; Blackwell: Oxford, UK, 1985.
44. McDonough, W.F.; Sun, S.S. Chemical evolution of the mantle. The composition of the Earth. *Chem. Geol.* **1995**, *120*, 223–253. [CrossRef]
45. Hanley, J.J.; MacKenzie, M.K.; Warren, M.R.; Guillong, M. Distribution and origin of platinum-group elements in alkalic porphyry Cu-Au and low sulfidation epithermal Au deposits in the Canadian Cordillera. In Proceedings of the 11th International Platinum Symposium, Sudbury, ON, Canada, 21–24 June 2010.
46. Chapman, R.; Allan, M.; Mortensen, J.; Wrighton, T.; Grimshaw, M. A new indicator mineral methodology based on a generic Bi-Pb-Te-S mineral inclusion signature in detrital gold from porphyry and low/intermediate sulfidation epithermal environments in Yukon Territory, Canada. *Miner. Depos.* **2017**, *53*, 1–20. [CrossRef]
47. Piestrzynski, A.; Schmidt, S.; Franco, H. Pd-minerals in the Santo Tomas II porphyry copper deposit, Tuba Benguet, Philippines. *Miner. Pol.* **1994**, *25*, 12–31.
48. Bogdanov, K.; Filipov, A.; Kehayov, R. Au–Ag–Te–Se minerals in the Elatsite porphyry-copper deposit, Bulgaria. *Geochem. Mineral. Petrol.* **2005**, *43*, 13–19.
49. Berzina, A.; Sotnikov, V.I.; Economou-Eliopoulos, M.; Eliopoulos, D.G. First finding of merenskyite (Pd,Pt)Te_2 in porphyry Cu-Mo ores in Russia. *Russ. Geol. Geophys.* **2007**, *48*, 656–658. [CrossRef]

50. Plotinskaya, O.Y.; Azovskova, O.B.; Abramov, S.S.; Groznova, E.O.; Novoselov, R.; Seltmann, K.A.; Spratt, J. Precious metals assemblages at the Mikheevskoe porphyry copper deposit (South Urals, Russia) as proxies of epithermal overprinting. *Ore Geol. Rev.* **2018**, *94*, 239–260. [CrossRef]
51. González-Jiménez, J.M.; Piña, R.; Kerestedjian, T.N.; Gervilla, F.; Borrajo, I.; Pablo, J.F.; Proenza, J.A.; Tornos, F.; Roqué, J.; Nieto, F. Mechanism for Pd-Au enrichment in porphyry-epithermal ores of the Elatsite deposit, Bulgaria. *J. Geochem. Explor.* **2021**, *220*, 106664. [CrossRef]
52. Lefort, D.; Hanley, J.J.; Guillong, M. Sub-epithermal Au-Pd mineralization associated with an alkalic porphyry Cu–Au deposit, Mount Milligan, Quesnel Terrane, British Columbia, Canada. *Econ. Geol.* **2011**, *106*, 781–808. [CrossRef]
53. Economou-Eliopoulos, M.; Eliopoulos, D.G. Palladium, platinum and gold concentrations in porphyry copper systems of Greece and their genetic significance. *Ore Geol. Rev.* **2000**, *16*, 59–70. [CrossRef]
54. Economou-Eliopoulos, M.; Eliopoulos, D. Platinum, palladium and gold content in the porphyry-Cu systems of the Vertiskos formation, Serbo-Macedonian Massif. *Bull. Geol. Soc. Greece XXVIII* **1993**, *2*, 393–405.
55. Sotnikov, V.I.; Berzina, A.N.; Economou-Eliopoulos, M.; Eliopoulos, D.G. Palladium, platinum and gold distribution in porphyry Cu±Mo deposits of Russia and Mongolia. *Ore Geol. Rev.* **2001**, *18*, 95–111. [CrossRef]
56. Dragov, P.; Petrunov, R. Elatsite porphyry copper-precious metals (Au and PGE) deposit. In *Plate Tectonic Aspects of the Alpine Metallogeny in the Carpatho-Balkan Region*; Proceedings, Annual Meeting UNESCO-IGCP Project; Popov, P., Ed.; USGS: Reston, VA, USA, 1996; Volume 356, pp. 171–174.
57. Hikov, A. Geochemistry of hydrothermally altered rocks from the Assarel porphyry copper deposit, Central Srednogorie. *Geol. Balc.* **2013**, *42*, 3–28.
58. Nixon, G.T. *Platinum-Group Elements in the Afton Cu-Au Porphyry Deposit, Southern British Columbia*; British Columbia Geological Survey Geological Fieldwork: Victoria, BC, Canada, 2004; pp. 263–290.
59. Thompson, J.F.H.; Lang, J.R.; Stanley, C.R. Platinum Group Elements in Alkaline Porphyry Deposits, British Columbia. In *Geological Fieldwork 2001*; British Columbia Geological Survey: Victoria, BC, Canada, 2001; pp. 57–64.
60. Ross, K.V.; Godwin, C.I.; Bond, L.; Dawson, K.M. Geology, alteration and mineralization in the Ajax East and Ajax West deposits, southern Iron Mask Batholith, Kamloops, British Columbia. In *Porphyry Deposits of the Northwestern Cordillera of North America*; Schroeter, T.G., Ed.; Canadian Institute of Mining, Metallurgy and Petroleum: Westmount, QC, Canada, 1995; Volume 46, pp. 565–580.
61. McInnes, B.I.A.; Cameron, E.M. Carbonated, alkaline hybridizing melts from a sub-arc New Guinea. *Earth Planet. Sci. Lett.* **1994**, *122*, 125–141. [CrossRef]
62. Keith, J.D.; Christiansen, E.H.; Maughan, D.T.; Waite, K.A. *The Role of Mafic Alkaline Magmas in Felsic Porphyry-Cu and Mo Systems*; Short Courses—Mineralogical Association of Canada: Quebec, QC, Canada, 1998; pp. 211–243.
63. Hanley, J.J. The Aqueous Geochemistry of the Platinum-Group Elements (PGE) in Surficial, Low-T Hydrothermal and High-T Magmatic Hydrothermal Environments. In *Exploration for Platinum-Group Element Deposits*; Mungall, J.E., Ed.; Mineralogical Association of Canada: Quebec, QC, Canada, 2005; pp. 35–56.
64. Zhu, J.-J.; Hu, R.; Bi, X.-W.; Hollings, P.; Zhong, H.; Gao, J.-F.; Pan, L.-C.; Huang, M.-L.; Wang, D.-Z. Porphyry Cu fertility of eastern Paleo-Tethyan arc magmas: Evidence from zircon and apatite compositions. *Lithos* **2022**, *424–425*, 106775. [CrossRef]
65. Sullivan, N.A.; Zajacz, Z.; Brenan, J.M.; Tsay, A. The solubility of platinum in magmatic brines: Insights into the mobility of PGE in ore-forming environments. *Geochim. Cosmochim. Acta* **2021**, *316*, 253–272. [CrossRef]
66. Berzina, A.P.; Gimon, V.O. Paleozoic–Mesozoic Porphyry Cu(Mo) and Mo(Cu) Deposits within the Southern Margin of the Siberian Craton: Geochemistry, Geochronology, and Petrogenesis (a Review). *Minerals* **2016**, *6*, 125. [CrossRef]
67. Moritz, R.; Kouzmanov, K.; Petrunov, R. Upper Cretaceous Cu–Au epithermal deposits of the Panagyurishte district, Srednogorie zone, Bulgaria. *Swiss Bull. Mineral. Petrol.* **2004**, *84*, 79–99.
68. Strashimirov, S.; Petrunov, R.; Kanazirski, M. Mineral associations and evolution of hydrothermal systems in porphyry copper deposits from the Central Srednogorie zone (Bulgaria). *Miner. Depos.* **2002**, *37*, 587–598. [CrossRef]
69. Kehayov, R.; Bogdanov, K.; Fanger, L.; Von Quadt, A.; Pettke, T.; Heinrich, C. The fluid chemical evolution of the Elatsite porphyry Cu-Au-PGE deposit, Bulgaria. In Proceedings of the 7th Biennial SGA Meeting "Mineral Exploration and Sustainable Development", Athens, Greece, 24–28 August 2003; Eliopoulos, D., Baker, T., Barriga, F., Beaudoin, G., Benardos, A., Boni, M., Borg, G., Bouchot, V., Brown, A., Christidis, G., et al., Eds.; Millpress: Rotterdam, The Netherlands, 2003; pp. 1173–1176.
70. Von Quadt, A.; Peytcheva, I.; Kamenov, B.; Fanger, L.; Heinrich, C.A.; Frank, M. The Elatsite porphyry copper deposit in the Panagyurishte ore district, Srednogorie zone, Bulgaria: U–Pb zircon geochronology and isotope-geochemical investigations of magmatism and ore genesis. *Geol. Soc. Lond. Spec. Publ.* **2002**, *204*, 119–135. [CrossRef]
71. Cheng, Z.G.; Zhang, Z.C.; Turesebekov, A.; Nurtaev, B.S.; Xu, L.J.; Santosh, M. Petrogenesis of gabbroic intrusions in the Valerianov-Beltau-Kurama magmatic arc, Uzbekistan: The role of arc maturity controlling the generation of giant porphyry Cu—Au deposits. *Lithos* **2018**, *320–321*, 75–92. [CrossRef]
72. Liu, B.X.; Zhang, Z.C.; Cheng, Z.G.; Xie, Q.H.; Turesebekov, A.; Nurtaev, B.; Santosh, M. Platinum group elements in gabbroic intrusions from the Valerianov-Beltau-Kurama arc: Implications for genesis of the Kalmakyr porphyry Cu–Au deposit. *Geol. J.* **2020**, *56*, 46–59. [CrossRef]
73. Pe-Piper, G.; Piper, D.J.W. Unique features of the Cenozoic igneous rocks of Greece. *Geol. Soc. Am.* **2006**, *409*, 259–282.

74. Pe-Piper, G.; Piper, D.J.W.; Koukouvelas, I.; Dolansky, L.M.; Kokkalas, S. Postorogenic shoshonitic rocks and their origins by melting underplated basalts: The Miocene of Limnos, Greece. *Geol. Soc. Am. Bull.* **2009**, *121*, 39–54. [CrossRef]
75. Park, J.W.; Campbell, I.H.; Malaviarachchi, S.P.; Cocker, H.; Hao, H.; Kay, S.M. Chalcophile element fertility and the formation of porphyry Cu ± Au deposits. *Miner. Depos.* **2019**, *54*, 657–670. [CrossRef]
76. Stein, H.J. Genetic traits of climax-type granites and molybdenum mineralization, Colorado Mineral Belt. *Recent Adv. Geol. Granite-Relat. Miner. Depos.* **1988**, *39*, 394–401.
77. Klemm, L.M.; Pettke, T.; Heinrich, C.A. Fluid and source magma evolution of the Questa porphyry Mo deposit, New Mexico, USA. *Miner. Depos.* **2008**, *43*, 533–552. [CrossRef]
78. Delibaş, O.; Moritz, R.; Chiaradia, M.; Selby, D.; Ulianov, A.; Revan, M.K. Post-collisional magmatism and ore-forming systems in the Menderes massif: New constraints from the Miocene porphyry Mo-Cu Pınarbaşı system, Gediz-Kütahya, western Turkey. *Miner. Depos.* **2017**, *52*, 1157–1178. [CrossRef]
79. Sillitoe, R.H. Gold-rich porphyry deposits; descriptive and genetic models and their role in exploration and discovery. *Rev. Econ. Geol.* **2000**, *13*, 315–345.
80. Richards, J.P. Tectono-magmatic precursors for porphyry Cu–(Mo–Au) deposit formation. *Econ. Geol.* **2003**, *98*, 1515–1533. [CrossRef]
81. Zhu, D.C.; Wang, Q.; Weinberg, R.F.; Cawood, P.A.; Chung, S.L.; Zheng, Y.F.; Zao, Z.; Hou, Z.Q.; Mo, X.X. Interplay between oceanic subduction and continental collision in building continental crust. *Nat. Commun.* **2022**, *13*, 7141. [CrossRef]
82. Zaccarini, F.; Pushkarev, E.V.; Fershtater, G.B.; Garuti, G. Composition and mineralogy of PGE-rich chromitites in the Nurali lherzolite gabbro complex, southern Urals, Russia. *Can. Miner.* **2004**, *42*, 545–562. [CrossRef]
83. Grieco, G.; Diella, V.; Chaplygina, N.L.; Savelieva, G.N. Platinum group elements zoning and mineralogy of chromitites from the cumulate sequence of the Nurali massif (southern Urals, Russia). *Ore Geol. Rev.* **2007**, *30*, 257–276. [CrossRef]
84. Bussolesi, M.; Zaccarini, F.; Grieco, G.; Tzamos, E. Rare and new compounds in the Ni-Cu-Sb-As system: First occurrence in the Gomati ophiolite, Greece. *Period Miner.* **2020**, *89*, 63–76.
85. Arai, S.; Uesugi, J.; Ahmed, A.H. Upper crustal podiform chromitite from the northern Oman ophiolite as the stratigraphically shallowest chromitite in ophiolite and its implication for Cr concentration. *Contrib. Miner. Petrol.* **2004**, *147*, 145–154. [CrossRef]
86. Robinson, P.T.; Bai, W.J.; Malpas, J.; Yang, J.S.; Zhou, M.F.; Fang, Q.S.; Hu, X.F.; Cameron, S.; Staudigel, H. Ultra-high pressure minerals in the Luobusa Ophiolite, Tibet, and their tectonic implications. *Geol. Soc. Lond. Spec. Publ.* **2014**, *226*, 247–271. [CrossRef]
87. Xiong, F.; Yanga, J.; Xua, X.; Kapsiotis, A.; Haoe, X.; Liuf, Z. Compositional and isotopic heterogeneities in the Neo-Tethyan upper mantle recorded by coexisting Alrich and Cr-rich chromitites in the Purang peridotite massif SW Tibet (China). *J. Asian Earth Sci.* **2018**, *159*, 109–129. [CrossRef]
88. Sideridis, A.; Tsikouras, B.; Tsitsanis, P.; Koutsovitis, P.; Zaccarini, F.; Hauzenberger, C.; Harilaos, T.; Hatzipanagiotou, K. Post-magmatic processes recorded in bimodal chromitites of the East Chalkidiki meta-ultramafic bodies, Gomati and Nea Roda, Northern Greece. *Front. Earth Sci.* **2022**, *10*, 1031239. [CrossRef]
89. Audétat, A.; Pettke, T.; Heinrich, C.A.; Bodnar, R.J. Special Paper: The Composition of Magmatic-Hydrothermal Fluids in Barren and Mineralized Intrusions. *Econ. Geol.* **2008**, *103*, 877–908. [CrossRef]
90. Halter, W.E.; Pettke, T.; Heinrich, C.A. The origin of Cu/Au-ratios in porphyry-type ore deposits. *Science* **2002**, *296*, 1844–1846. [CrossRef]
91. Beane, R.E.; Titley, S.R. Porphyry copper deposits, Part II. Hydrothermal alteration and mineralization. *Econ. Geol.* **1981**, *75*, 214–235.
92. Sun, W.; Huang, R.; Liang, H.; Ling, M.; Li, C.; Ding, X.; Zhang, H.; Yang, X.; Ireland, T.; Fan, W. Magnetite–hematite, oxygen fugacity, adakite and porphyry copper deposits: Reply to Richards. *Geochim. Cosmochim. Acta* **2014**, *126*, 646–649. [CrossRef]
93. Dilles, J.H.; Kent, A.J.R.; Wooden, J.L.; Tosdal, R.M.; Koleszar, A.; Lee, R.G.; Farmer, L.P. Zircon compositional evidence for sulfur-degassing from ore-forming arc magmas. *Econ. Geol.* **2015**, *110*, 241–251. [CrossRef]
94. Prichard, H.; Economou-Eliopoulos, M.; Fisher, P.C. Contrasting Platinum-group mineral assemblages from two different podiform chromitite localities in the Pindos ophiolite complex, Greece. *Can. Mineral.* **2008**, *46*, 329–341. [CrossRef]
95. Bonev, N.; Dilek, Y.; Hanchar, J.; Bogdanov, K.; Klain, L. Nd–Sr–Pb isotopic composition and mantle sources of Triassic rift units in the Serbo-Macedonian and the western Rhodope massifs (Bulgaria–Greece). *Geol. Mag.* **2012**, *149*, 146–152. [CrossRef]
96. Blanks, D.E.; Holwell, D.A.; Fiorentini, M.L.; Moroni, M.; Giuliani, A.; Tassara, S.; González-Jiménez, J.M.; Boyce, A.J.; Ferrari, E. Fluxing of mantle carbon as a physical agent for metallogenic fertilization of the crust. *Nat. Commun.* **2020**, *11*, 4342. [CrossRef]
97. Lips, A.l.W.; Herrington, R.J.; Stein, G.; Kozelj, D.; Popov, K.; Wijbrans, J.R. Refining of porphyry copper formation in the Serbian and Bulgarian portions of the Cretaceous Carpath-balkan belt. *Econ. Geol.* **2004**, *99*, 601–609. [CrossRef]